ACOUSTIC PERTURBATION OF A NEON GLOW DISCHARGE

JOEL LEE CRANDALL, JR.

[redacted]

ACOUSTIC PERTURBATION

OF A

NEON GLOW DISCHARGE

by

Joel Lee Crandall, Jr.
Lieutenant, United States Navy
B. Aero. E., The Ohio State University, 1959

Submitted in partial fulfillment
of the requirements
for the degree of

DOCTOR OF PHILOSOPHY

from the

UNITED STATES NAVAL POSTGRADUATE SCHOOL
March 1967

ABSTRACT

Acoustic waves of finite extent were propagated into a dc glow discharge. It was found that compression phases of these waves reduced light emitted by the discharge, while rarefaction phases increased this light. In the compression phase of the acoustic wave these changes were attributed to increased losses of electron energy through an increase in the collision frequency. Electron energy was increased in the rarefaction phase of the acoustic wave as collision frequency was reduced.

Fast and slow waves of stratification were excited by the acoustic waves. These waves of stratification had opposite signs of light intensity variation when excited by compression and rarefaction phases of the acoustic wave.

TABLE OF CONTENTS

Chapter		Page
I	INTRODUCTION	7
II	EXPERIMENTAL APPARATUS	14
III	ACOUSTIC WAVE INTERACTIONS	26
	Translation of Gas	26
	Interaction in a Homogeneous Positive Column	31
	Interaction in an Inhomogeneous Positive Column	36
IV	ANALYSIS OF ACOUSTIC INTERACTIONS IN THE DISCHARGE	45
	Change of Electron Temperature	45
	Excitation of Acoustic Waves by the Discharge	51
Appendix		
I	DISCHARGE PROCESSES	57
	General Description	57
	Cathode Fall	60
	Positive Column	63
II	WAVES OF STRATIFICATION	78
	Theory of the Wave of Stratification	78
	Striation Boundaries	94
	Waves of Stratification Excited by Acoustic Waves	97
	Irradiation of the Discharge	100
III	OTHER WORKS ON PLASMA-ACOUSTIC WAVE INTERACTIONS	109

LIST OF ILLUSTRATIONS

Figure		Page
1-1	Wave of stratification in time and time-space development.	9
2-1	Arrangement of equipment for acoustic experiments.	15
2-2	Current and pressure boundary of striation-free operation in tube used for acoustic experiments.	16
2-3	Time-space display showing the propagation of an acoustic wave in the discharge.	18
2-4	Diode current as a function of pressure, voltage constant.	20
2-5	Acoustic waves from high voltage pulse modulation and square wave modulation of exciting discharge current as recorded by diode microphone.	22
2-6	Difference in arrival times of acoustic waves as exciting discharge power is changed.	24
3-1	Light intensity as a function of position transverse to the discharge axis.	27
3-2	Light intensity variations produced by rarefaction and compression acoustic waves.	28
3-3	Light intensity variations at the cathode end of the discharge resulting from the acoustic waves, E3 cathode.	29
3-4	Light intensity variations at the cathode end of the discharge resulting from the acoustic waves, E4 cathode.	30
3-5	Time-space development of light intensity in a 1.3 torr, 2.6 mA discharge showing effect of anode to cathode propation of compression and rarefaction waves.	33
3-6	Time-space development of light intensity in a 2.2 torr, 3.1 mA discharge, showing anode to cathode propagation of acoustic waves produced by high-voltage pulser.	34
3-7	Time-space development of light intensity in a 0.82 torr, 35 mA neon discharge for anode to cathode propagation of an acoustic wave.	35
3-8	Light intensity as a function of position in a 0.82 torr, 15 mA neon discharge. Standing striations visible.	37

3-9	Time-space development of light intensity in a 0.82 torr, 10 mA neon discharge, showing anode to cathode propagation of acoustic waves and origin of striations from more than one point in the positive column.	39
3-10	Time-space development of light intensity in a 0.7 torr, 16 mA neon discharge. Anode to cathode propagation of acoustic waves.	40
3-11	Time-space development of light intensity in a 0.7 torr, 16 mA neon discharge. Cathode to anode propagation of acoustic waves.	42
3-12	Time-space development of light intensity in a 4.0 torr, 0.2 mA neon discharge. Cathode to anode propagation of acoustic waves.	43
4-1	Schematic of discharge showing light and dark areas with accompanying electric field.	58
4-2	Time-space diagram of solution to simplified system of equations describing the wave of stratification.	84
4-3.	Dispersion curves from zero- and infinite-Debye length theories.	92
4-4	Time-space development of waves of stratification in pure neon and in a neon-hydrogen mixture, showing convex and concave dispersion.	93
4-5	Current and pressure boundary of striation-free operation in tube I.	96
4-6	Light intensity and voltage drop across tube I as a function of current showing effects of irradiation by a second discharge.	103
4-7	Line drawing used in explanation of figure 4-6.	104
4-8	Waves of stratification in tube I showing change of dispersion under irradiation.	107

ACKNOWLEDGMENTS

A great many people have assisted in this work in a variety of ways. I would like to express my gratitude to:

Professor A. W. Cooper, my thesis advisor, for helpful guidance during the work - particularly in encouraging me to better formulate results.

Mr. William P. Jones, of the NASA Ames Laboratory, for suggesting the study of acoustic wave interactions.

Professor K-H. Woehler for a critical reading of this work.

Professor O. B. Wilson for his encouragement and for helpful discussions of the acoustic processes.

Professor F. Bumiller for the assistance given in pulse techniques.

Mr. Jan van Gastel, for his expert craftsmanship in the construction of several complex discharge tubes.

My family, for their patience with the long hours spent away from home.

My wife, Sara, for her encouragement during several non-productive periods of the experiment, and for typing the dissertation.

CHAPTER I

INTRODUCTION

Electric and magnetic fields have been widely used for investigation of the properties of glow discharges because of their strong interaction with charged particles. In recent years, the interaction of acoustic waves with the discharge plasma has received some attention. These experiments have been limited in scope and little theoretical work has accompanied them. This work is an experimental study of the effects of an acoustic wave group of finite extent upon a neon glow discharge 40 cm long, in a 2.5 cm diameter tube in the pressure range 0.7 to 4.0 torr, and operated at currents up to 35 ma.

In the discharge of electricity through low pressure noble gases, spontaneous oscillations of the discharge current are nearly always observed. Frequencies of these oscillations range from 0.5 to 50 kHz. Photomultiplier signals indicate that the light intensity of the positive column also oscillates with this frequency. These oscillations are caused by the anode to cathode motion of light areas in the discharge which are known as moving striations.

Studies of moving striations have made great progress in recent years by investigating transients introduced into a homogeneous discharge through impulsive modulation of the current, or through application of a high voltage pulse to a ring encircling part of the positive column. These transients have the form of a wave group or wave packet which propagates toward the anode with a group velocity u, while the component waves have phase velocity v directed toward the cathode. It is therefore a backward wave. Individual waves have the characteristics of moving striations, and the group has been termed a "wave of stratification".

Figure 1-1 shows schematically the traces observed by a photomultiplier at two points in the column (1-1(a), (b)). From these the propagation in the direction of the anode can be seen. Part (c) of this figure shows development of the wave of stratification in time and space, with positive X chosen in the direction of the electric field. In this diagram, the dark areas correspond to the moving striations which are present within a wave packet. Striation motion toward the cathode is evident, and the striation amplitude is depicted by the width of the line.

Under conditions in which this wave receives large amplification during propagation along the column, the oscillations of current which occur as it arrives at the anode cause excitation of additional waves of stratification. Further increase of the amplification causes the striations to be self-excited, with striations of largest amplitude appearing at the anode end of the discharge.

Pekarek first reported these waves in 1954, and his ensuing theoretical and experimental works have established several important characteristics: [41]

1) the waves are ionization phenomena, dependent upon the change of ionization rate with electron temperature;

2) a single slow and two fast waves exist, with the slow wave dependent upon stepwise ionization, the fast waves on direct ionization;

3) the slower of the fast waves is associated with motion of an atomic ion, the faster with the motion of a molecular ion;

4) any localized perturbation of ionization rate of sufficient amplitude will cause the wave to originate; perturbations of opposite sign produce waves with opposite courses of light intensity;

5) the formation of space charges due to higher mobility of

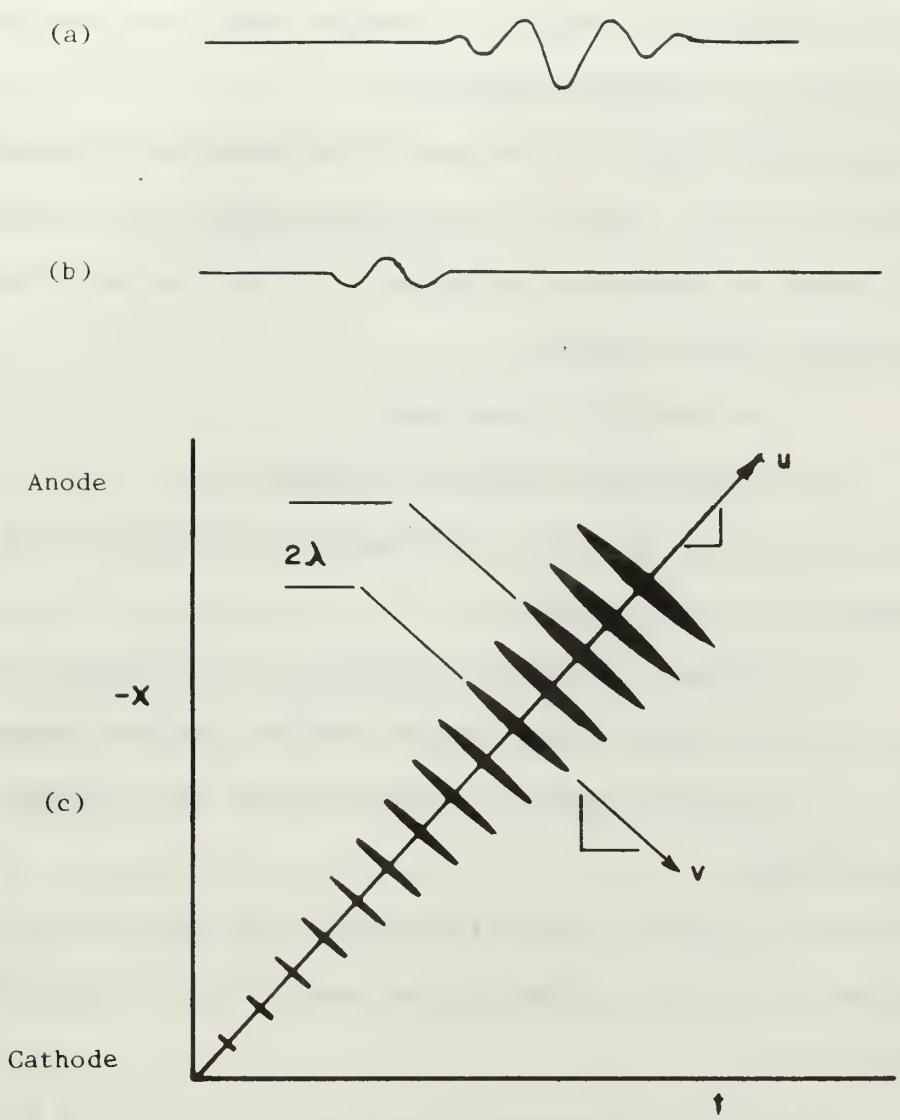

Figure 1-1. (a) Time modulation of light intensity in anode region by wave of stratification.

(b) Time modulation of light intensity nearer cathode.

(c) Time-space development of light intensity by wave of stratification.

the electrons, and the consequent change of electron temperature, cause the wave to propagate;

6) striations with small separation (or wavelength, λ) are damped by longitudinal ambipolar diffusion, those with long wavelength by relaxation of electron temperature.

Pekarek has shown that any spatial perturbation of the steady-state ion density causes a localized space-charge region to be formed. [53] On this basis the formation and motion of striations can be explained by the following chain of events:

a) ion density is increased;

b) a space charge region is formed;

c) electric field is increased on the anode side of this region, decreased on the cathode side;

d) electron temperature changes with the electric field, causing

e) increase of light toward cathode, decrease toward anode;

f) ions move toward the cathode under the influence of the main electric field.

Propagation of the wave toward the anode can be explained by considering the decrease of electric field on the anode side of this disturbance. In this case:

g) electron temperature and ionization rate are decreased, causing

h) a reduction of light intensity and a negatively charged region;

i) this region of negative charge enhances the electric field on its anode side, causing

j) increase of ionization rate and ion density.

Step (j) was the initial condition of the disturbance. Since the first ion density perturbation caused a second similar region to form on the anode side, repetition of this cycle describes propagation of the wave in the direction of the anode.

Properties of the wave can be related to microphysical processes in the discharge through the relaxation time which is defined as

$$\tau_o = \frac{\lambda}{2} \cdot \frac{1}{u + v} \qquad (1)$$

This relaxation time is characteristic of the slowest process in the chain of events which form and propagate the wave.

In the case of the fast wave, it is the time required for the excess space charge to vanish through diffusion losses, while in the slow wave it is the sum of this diffusion time and the time required to ionize the excess of ions produced by the increase of electron temperature.

Dispersion of this wave in the inert gases is such that the higher frequency components of the packet generally appear earliest at a given position. In time-space photographs, this type of dispersion causes the striation paths to be curved convex with respect to origin.

Amplification of the wave is dependent upon the change of ionization rate with temperature, and upon the spatial phase difference between the course of electric field variation and that of the electron temperature. [52]

Thus the essential properties of the wave of stratification are well understood. Detailed mathematical formulation of the wave of stratification has been carried out by Pekarek and various co-workers [41 - 60], and the theory for the case of zero Debye length has been found to describe this case reasonably well. However, all perturbation work has

been accomplished electrically with the exception of some work by Sicha et. al., who used square-wave modulation of the power input to re-entrant RF cavities to excite the wave of stratification, thus directly perturbing the ion density locally. [73] Other areas of the column are affected, however, as standing striations form between the point of application of the RF discharge and the anode. These are similar to those found at the cathode end of the positive column. Both the high voltage pulses and pulse modulation of the current also cause disturbance of the discharge over large areas.

There has been no reported attempt to excite waves of stratification by magnetic fields, by the use of radiation, or by acoustic waves. In the acoustic work which has been performed in dc discharges, Subertova has reported creating standing striations by the use of acoustic waves. [80] Carretta and Moore observed acoustic waves which they attributed to moving striations [9], although these were later shown to originate in the cathode region of the discharge, and attributed to changes in gas heating as discharge current was changed. [83] Saxton investigated the influence of acoustic waves on the positive column and found that the amplitude of the electron density variation was proportional to the neutral gas density variation. [11, 12] Wojaczek observed that a pulse discharge at one end of the main discharge caused acoustic waves which modulated the intensity of the light emitted from the positive column. [87]

With the exception of a brief explanation by Saxton, there has been no analysis of the acoustic interactions by the authors of these works. Several other experiments involving acoustic waves have been performed, but none have involved dc discharges. Ingard has theoretically analyzed

the possibilities of producing acoustic waves from interaction with charged particles, but has given little consideration to the inverse problem. [27]

The way is clearly open for an extensive investigation of the effect of acoustic waves on the positive column of a dc discharge.

In this work, a pulse discharge is used to excite acoustic waves of finite extent. Amplitude of these waves is measured by a thermionic gas-filled diode, and interaction in the positive column of the discharge is observed with a photomultiplier tube and displayed on time-space photographs. [14,76]

A theoretical explanation of the interaction of acoustic waves in the positive column is given.

CHAPTER II

EXPERIMENTAL APPARATUS

Figure 2-1 shows the arrangement of equipment used in this experiment. Acoustic waves were excited by a discharge operated between electrodes E1 and E2, and observed in the dc discharge between electrodes E3 and E4. The exciting discharges were produced by high voltage pulses in most cases. Square wave modulation of the discharge current was used to compare the effect of propagating a compression or a rarefaction phase as the leading component of the wave. Hollow cylinders with diameter 18 mm were employed to take advantage of the higher efficiency and higher current densities which characterize the hollow cathode effect. [62, 63, 78, 79] Cross-sectional area is small, giving minimum interference with the propagation of acoustic waves. Electrode E1 was always used as the cathode of the exciting discharge; polarity of the electrodes in the observing discharge could be reversed easily to study effect of direction of propagation in the discharge.

Power for the observing discharge was provided by a 0-1 kv supply, the working load was a pentode with indirectly heated cathode (RCA 807). This was chosen to give ripple-free operation of discharge current. Variable resistors were used in the cathode circuit, allowing the grid to be biased negatively by current flow and the operating current to be selected by this simple change of resistance. A pentode was selected as the discharge load since this has been shown to increase the range of current in which the discharge is striation-free. [44] Figure 2-2 shows the current and pressure boundary of striation-free operation. A curve calculated from the empirical relations in [69] is also shown. For a given pressure, both the upper and lower current boundaries of this region

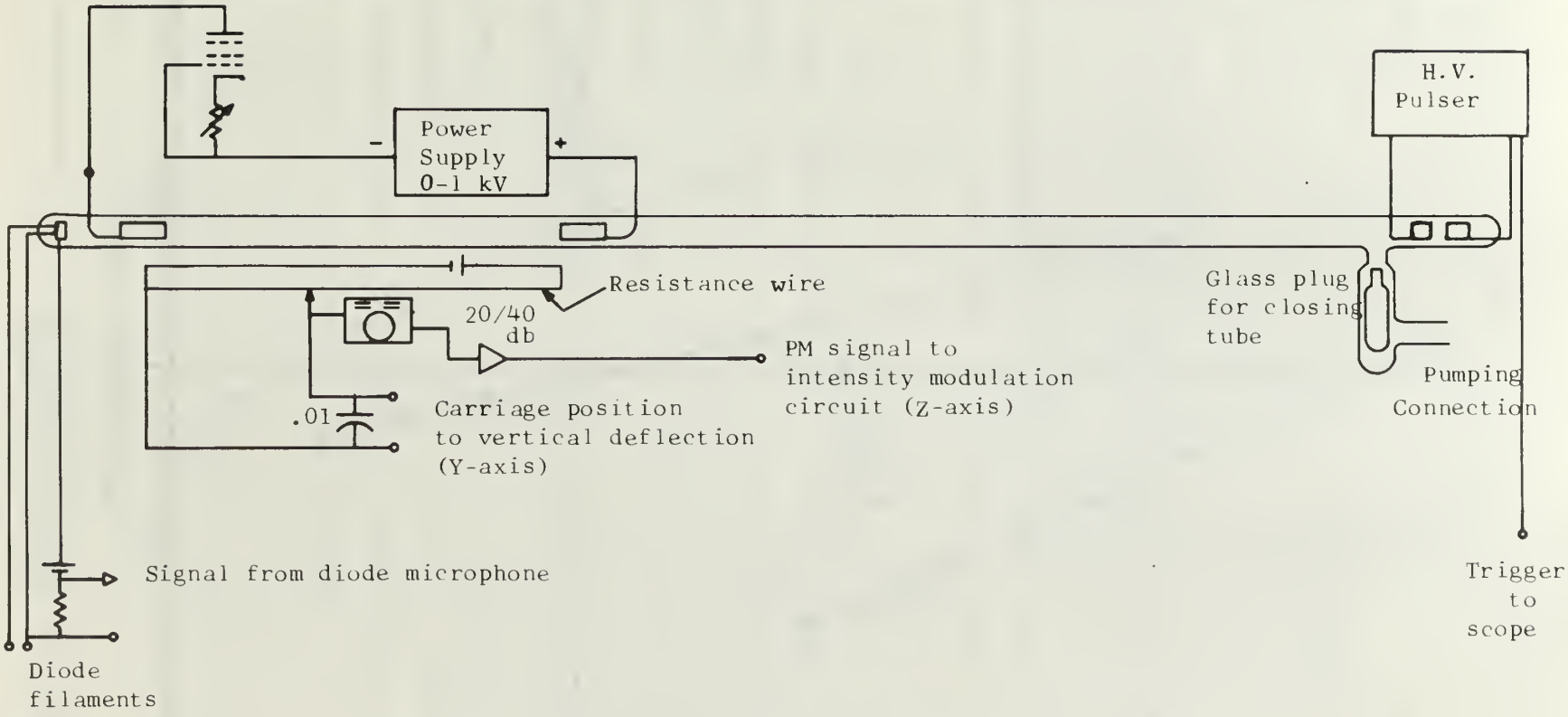

Figure 2-1. Experimental arrangement, showing Z-modulation and diode circuits.

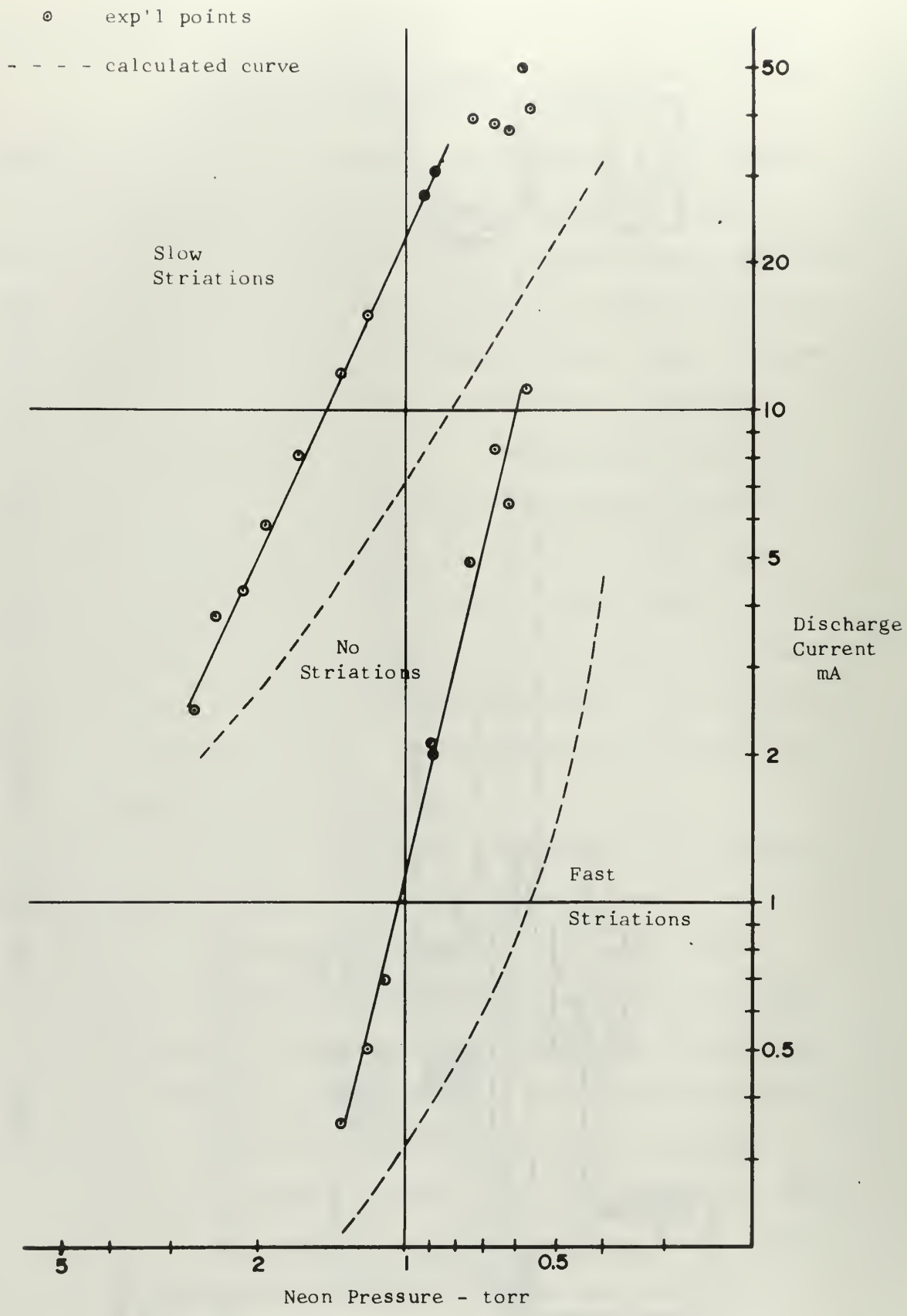

Figure 2-2. Striation boundaries in a 2.5 cm diameter, 40 cm long Neon discharge.

were found to be larger than the values given by the empirical relations. Formulae for these relations are given in Appendix II.

For observing the interaction in the discharge, the time-space display method described by Stirand, et. al., was employed (Figure 2-1). [76] In this technique, the oscilloscope horizontal sweep is triggered by the exciting discharge, vertical position of the trace corresponds to position of the photomultiplier along the column, and the intensity of the beam is modulated by the photomultiplier signal. With the carriage at a given position, variation of intensity of the trace indicates a time-varying phenomenon. When the carriage is moved to a new position, the vertical position of the trace is changed. These variations occur at different times for phenomena which propagate with finite velocities. A photograph taken with the shutter open while the carriage is moved slowly along the column, records the development in time and space of time-varying phenomena. Figure 2-3 is a time-space photograph showing the propagation of an acoustic wave from anode to cathode in the discharge tube. The anode is at the upper limit of the trace, the cathode at the lower limit and time increases to the right. Light intensity variations occur earlier at the anode end of the discharge because of the anode to cathode propagation. Photomultiplier output is at negative potential, causing photographs taken in this manner to show light intensity variations in an inverted manner, i.e., increases in light intensity in the discharge correspond to darker areas in the photograph. The unmodulated level of illumination of the oscilloscope screen was chosen such that very small variational signals could be observed. Frequency response of the intensity modulation circuit caused distortion of light intensity changes longer than about five milliseconds.

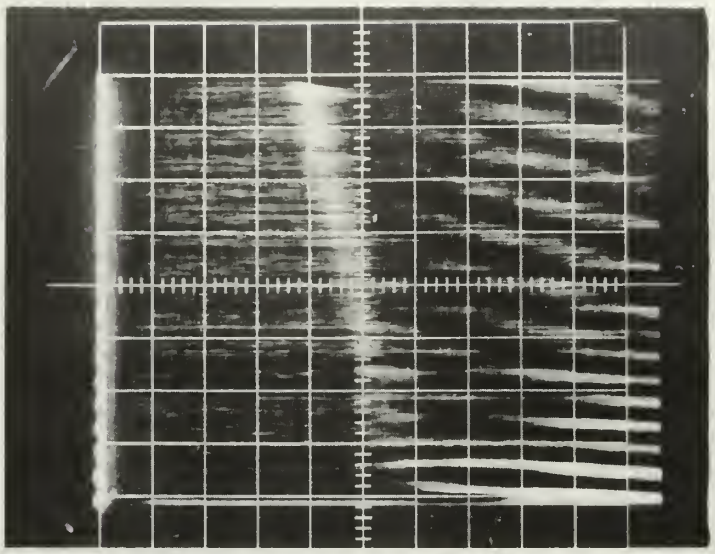

Figure 2-3. Time-space photograph showing propagation of an acoustic wave from anode to cathode in a 2.7 torr, 0.5 ma Neon discharge. Time scale is 0.5 msec/division.

Density variations in the acoustic waves were measured by recording changes in the conductivity of a gas-filled thermionic diode. This technique, first noted by Dayton, et. al. [14], is based upon mobility-limited operation of the diode according to the equation

$$i = KV^2. \tag{2}$$

Here K involves the mobility which is a function of neutral particle density. This device is calibrated by recording current as a function of pressure with voltage fixed. In this case, the density changes are directly related to pressure changes through the perfect gas law, as temperature is also held constant. The functional dependence of current upon pressure can therefore be expressed as

$$i = \frac{a_1}{\rho^m}, \tag{3}$$

where the value of m is obtained from the curves of figure 2-4. Fractional density variations result in fractional current changes, which may be read as voltage variations across a resistor R:

$$\frac{d\rho}{\rho} = \frac{-di}{mi_o} = \frac{-dV}{m \cdot R \cdot i_o}. \tag{4}$$

From the data in figure 2-4, for a voltage of 20 volts m is 0.286, giving

$$\frac{d\rho}{\rho} = 3.47 \frac{dV}{i_o}, \tag{5}$$

with R = 1000 ohms, and i_o in ma.

In the acoustic waves, compressions and rarefactions are adiabatic, with pressure and density related through

$$\frac{p}{\rho^\gamma} = \text{const.} \tag{6}$$

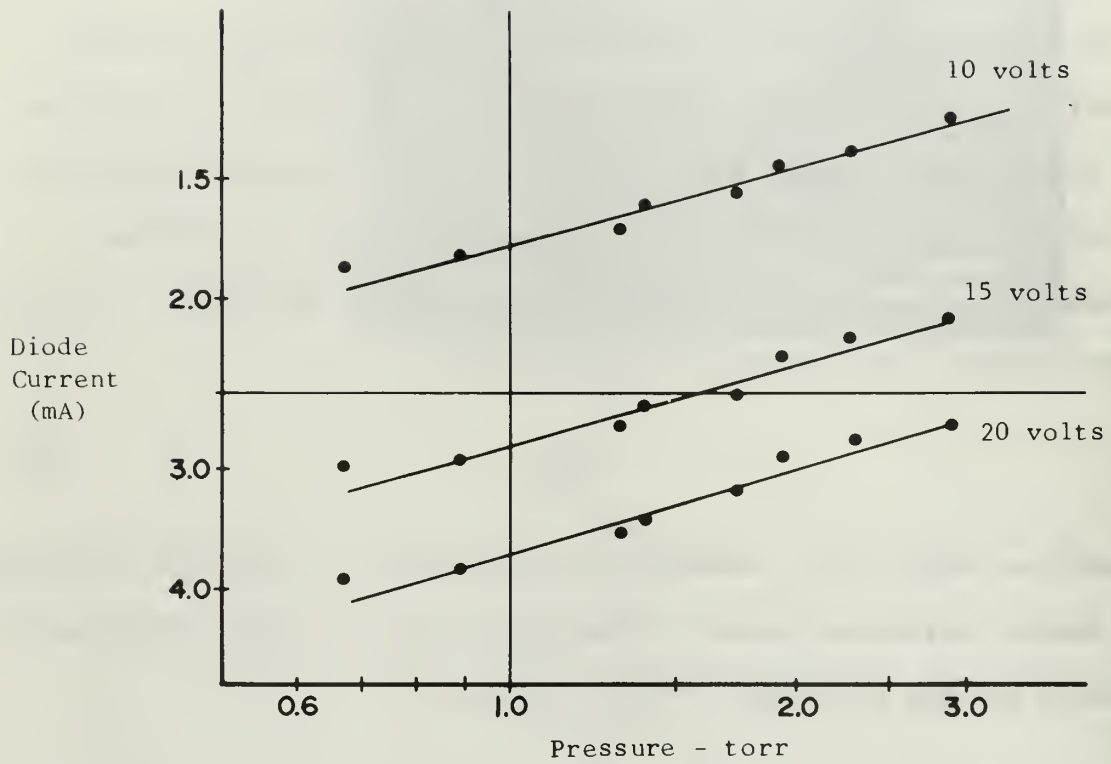

Figure 2-4. Diode current (multiplied by 2) as a function of pressure for constant plate voltage.

Thus

$$\frac{dp}{p} = \frac{d\rho}{\rho} \cdot \gamma \tag{7}$$

and the sensitivity of the device at 1.0 torr, with 20 volts from anode to cathode is

$$S = \frac{dV}{dp} = 0.24 \frac{mV}{\mu bar} . \tag{8}$$

Dayton's method gives a sensitivity of 0.79 mV/μbar in nitrogen at 1.0 torr. This can be attributed to the larger total collision cross-section of nitrogen. His calculation may be in error, however, as he seems to have assumed an isothermal relation between density and pressure instead of an adiabatic relation.

Experiments showed that operation of the neon-filled diode in the experimental pressure range was described by the equation

$$i = KV^{1.6} . \tag{9}$$

This indicates that the diode is nearly space-charge limited rather than mobility limited. The curve of figure 2-4 indicates that the variation of conductivity with pressure is sufficient to allow its use as a detector of density variation.

Acoustic wave amplitudes are expressed in fractional variations of neutral gas density, as it is these variations which will affect the properties of the plasma. All measurements of acoustic wave amplitudes were made with the observing discharge extinguished.

Figure 2-5 shows the diode signals for acoustic waves produced by the high voltage pulse discharge and by square wave modulation of the exciting discharge current by the pentode. Density increases are indicated by a negative change in voltage. In this figure it is evident

a

b

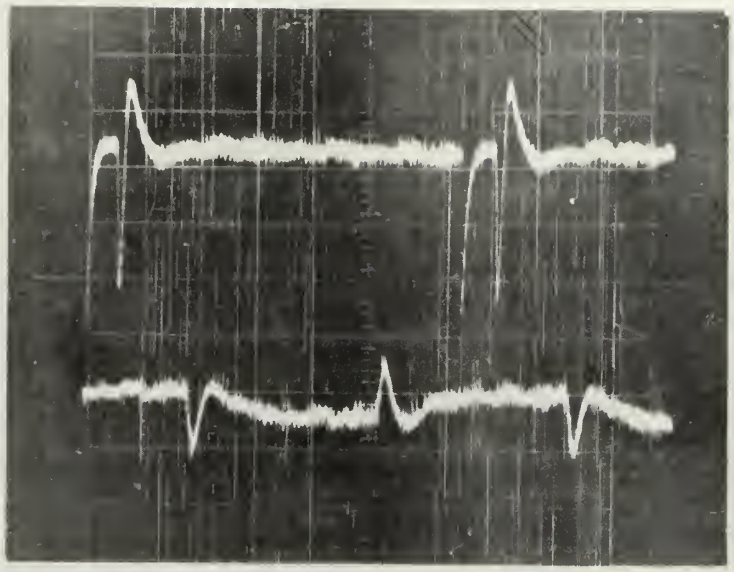

5 msec/division

Figure 2-5. (a) Acoustic wave produced by 2 kv on plate of high voltage pulser. Density variation is 0.27 per cent. (b) Acoustic wave produced by square wave modulation of discharge current. Peak density variation is 0.094 per cent, difference in static levels is 0.04 per cent.

that the high-voltage pulses excite waves of much larger amplitude and shorter rise time. Maximum density variation is 0.27 per cent for the larger amplitude acoustic wave, and 0.09 per cent for the smaller amplitude wave. A static density variation of 0.04 per cent is also created by square wave modulation of the discharge current.

Translation of the gas along the discharge tube axis by a sinusoidal acoustic wave is given by

$$\xi = \int_0^t C \cdot S_o \cdot \mathrm{Sin}\,\omega t \, dt$$

$$= \frac{CS_o}{\omega} (1 - \cos\omega t) , \qquad (10)$$

where

C = sonic velocity (456 m/sec @ 24°C)

S = condensation ($d\rho/\rho$).

For the high voltage pulser, a frequency of 1 kHz approximates the compression phase, and the maximum translation is 1.23 mm when the density variation is 0.27 per cent. In a later section, this is shown to be important.

Firing of the high voltage pulser causes an electrostatic interaction between the two discharges. This may result from capacitive coupling, or from the change in field configurations near electrodes as the pulses are initiated. In either case the mechanism is unclear, causing an increase in the signal detected in one instance and a decrease in another (figure 2-6).

Figure 2-6 shows the form of the acoustic waves detected by the diode for pulser voltages of 2 and 4 kv. This figure shows that the higher voltage pulse produces a larger electrostatic interaction, a

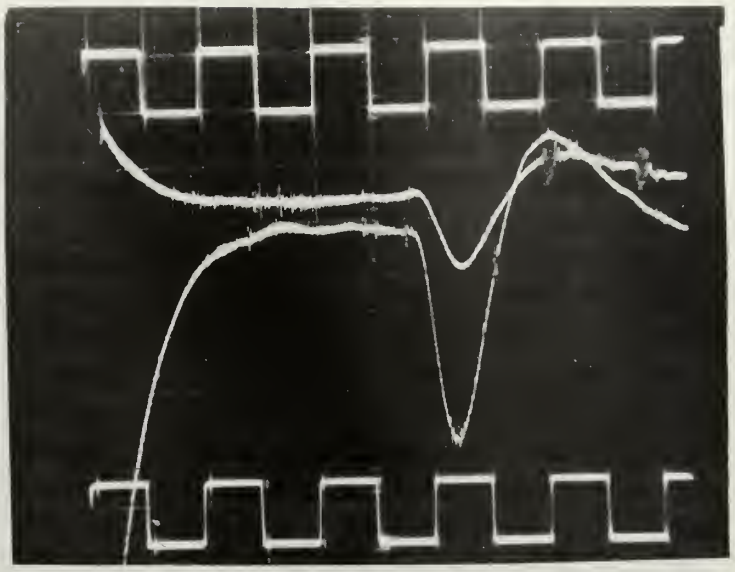

Figure 2-6. Traces (a) and (d) are 1001 Hz square waves used as base lines for calculation of acoustic wave velocity. Nominal time base is 0.5 msec/division. Traces (b) and (c) are the acoustic waves observed by the diode for pulser voltages of 2 and 4 kilovolts. Density increase is indicated by a downward deflection of the beam. Deflections prior to 2.5 msec are due to electrostatic interaction. The velocity of the acoustic wave in (b) is 440 m/sec, and for (c) is 448 m/sec, if acoustic waves are assumed to arise at the moment of maximum light intensity in the exciting discharge. Density variation in (b) is 0.34 per cent, and in (c) is 0.71 per cent.

larger amplitude acoustic wave, and an acoustic wave which arrives earlier. Propagation velocities of these two waves are 440 m/sec and 456 m/sec respectively, if the waves are assumed to originate at the time of breakdown of the gas. The latter velocity corresponds to the sonic velocity of small amplitude waves for a neutral gas temperature of 24°C. This apparent difference of propagation velocities cannot be resolved without a second diode in the tube or some other device to allow time of flight to be measured within the tube. If both waves are assumed to propagate with the same velocity, 75 microseconds are required for the formation of the acoustic wave by the smaller amplitude pulse.

Damping of acoustic waves by collisions and heat transfer to the walls predominates over collision and heat conductivity losses in the volume for the pressure range of this experiment. [25] The damping coefficient is of the order of 2×10^{-2} cm^{-1}.

CHAPTER III

ACOUSTIC WAVE INTERACTIONS

A. Translation of the Gas

Acoustic waves were propagated across a short discharge in another tube in order to show the translation of the gas caused by these waves. In figure 3-1, static light intensity in relative units is plotted as a function of distance from the centerline of the discharge. The shape of this curve is approximately Gaussian. Arrows indicate photomultiplier locations for traces (b) and (c) of figure 3-2.

Trace (a) of figure 3-2 shows the current in the exciting discharge as a function of time. The trace begins with a decrease of current, which causes a rarefaction wave to propagate due to the removal of a heat source. In trace (b), the photomultiplier is located toward the exciting discharge from the centerline of the observing discharge. This causes a brighter area to be moved in front of the slit as the acoustic wave arrives, while trace (c) shows opposite behavior of the light intensity as a darker area is moved in front of the photomultiplier. Effects are reversed in both traces as current in the exciting discharge is increased and a compression wave is propagated.

When the acoustic waves were propagated along the axis of the discharge tube, a similar effect was noted in the standing striations of cathode regions. However the light intensity was nearly square wave modulated when E4 was the cathode and the exciting discharge current was modulated by a square wave. The behavior with E3 as cathode was similar to that observed for propagation of the acoustic waves transverse to the discharge axis, and did not show this square wave modulation. Figures 3-3 and 3-4 show the waveforms observed when each of these electrodes

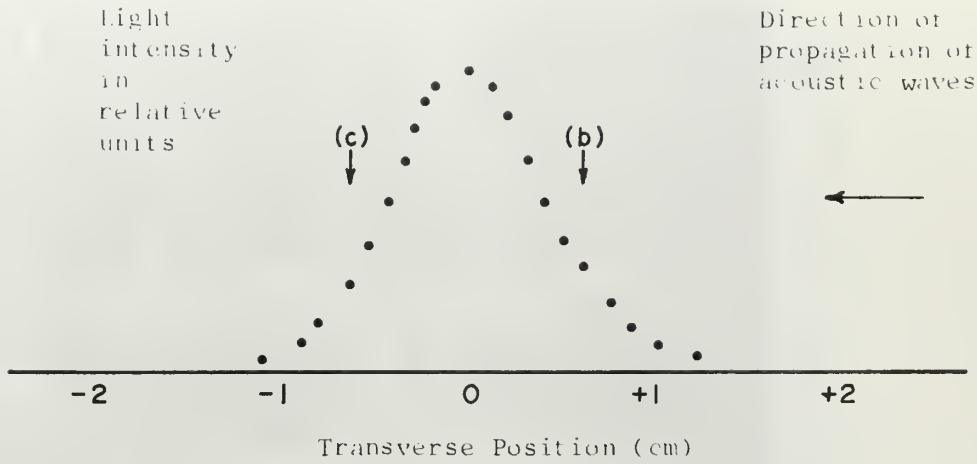

Figure 3-1. Light intensity as a function of position transverse to the positive column of an observing discharge. Arrows indicate location of the photomultiplier for traces (b) and (c) of figure 3 2. For this experiment, acoustic waves were propagated across the column (from right to left in this diagram).

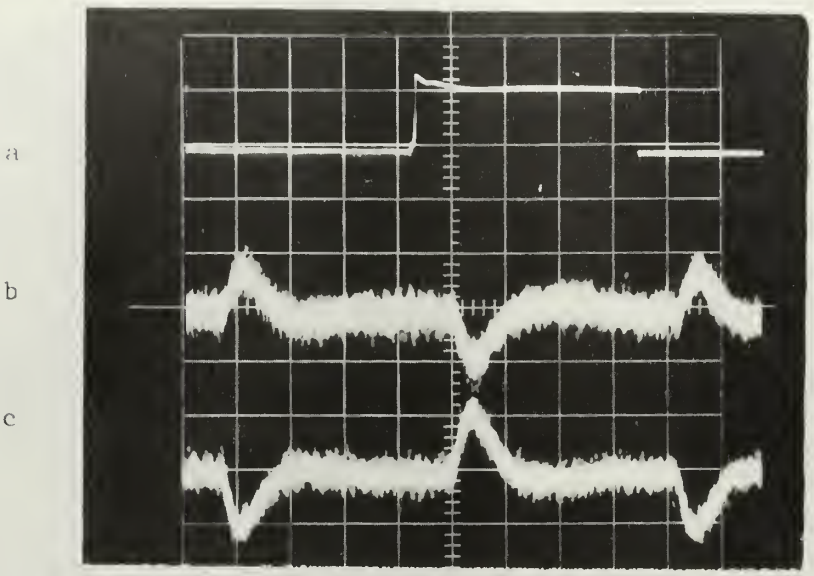

Figure 3-2. (a) Current variation in the exciting discharge as a function of time; 50 ma/division. (b) Light intensity variation on the side of the positive column of the observing discharge toward the exciting discharge. (c) Light intensity variation on the side of the positive column of the observing discharge away from the exciting discharge. Current in the observing discharge = 3.5 ma. Time base = 2 msec/division.

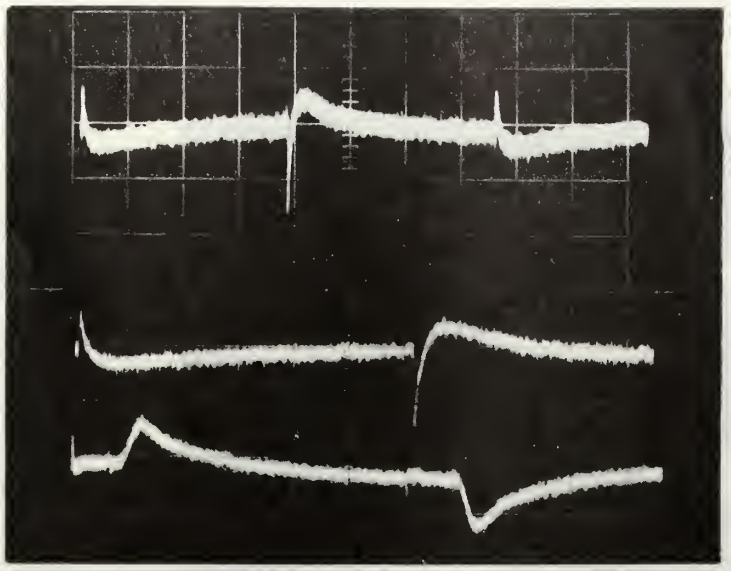

Figure 3-3. Light intensity variations on the cathode (exciting discharge) side of the first standing striation in the positive column of tube II. E3 is cathode, 0.7 torr, 16 ma. Time per division is shown to the right of each trace. Rarefaction wave arrives first in each case. All vertical scales are identical. Tube II is the tube used for acoustic experiments.

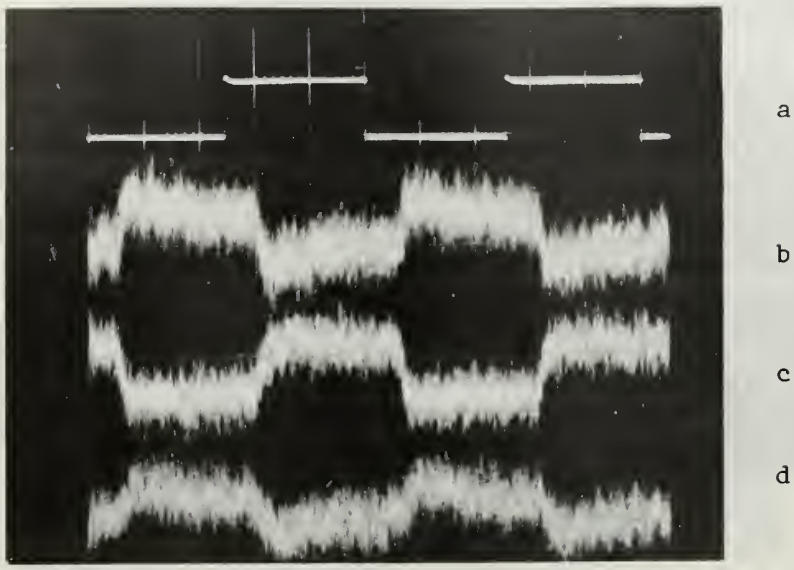

Figure 3-4. Light intensity variations in the head of the positive column as a function of time. Time scale: 5 msec/division. (a) Current variation in exciting discharge, 20 ma/division.(b) Anode side of first standing striation.(c) Cathode side of first standing striation. (d) Negative glow. E4 is cathode, 0.7 torr, 16 ma. Rarefaction wave propagated first.

is operated as cathode. Figure 3-3 also shows that approximately 150 msec is required for light intensity to return to the original value. Amplitude of the compression phase of the wave is decreased as frequency of the modulating square wave is increased.

No satisfactory explanation has been found for the nearly square wave modulation of light intensity in the cathode regions when E4 is used as cathode. This occurred only when current of the exciting discharge was square wave modulated.

B. Interaction in a Homogeneous Positive Column

Time-space photographs are extensively used in this section to present the several effects which were observed when acoustic waves were propagated through the discharge. For these photographs, electrode E3 is always located at the upper limit of the trace, electrode E4 at the lower. Travel of the photomultiplier is 40 cm in all cases, with inter-electrode separation 39 cm, and approximately equal overlap at each end of the carriage travel.

The translation of gas discussed in the preceding section gives rise to large variations of light output for regions of the discharge having standing striations. A standing striation is always located at the head of the positive column, and other standing striations which may be present are damped in the direction of the anode. Damping is increased as current is reduced, leaving the column nearly homogeneous over 3/4 of its length for currents below about 2 ma.

Interaction in the positive column is first examined by using acoustic waves generated from square wave modulation of the exciting discharge current, and secondly with the larger amplitude acoustic waves from the high voltage pulser. In the first case, the general effect of

compression and rarefaction waves upon the column is established, while with the larger pulse an additional effect is observed.

Figure 3-5 shows anode to cathode propagation of acoustic waves produced by square wave modulation of the exciting discharge. A rarefaction wave is propagated first in all experiments with the square wave modulation technique, and it is seen that this rarefaction causes an increase in light emitted by the discharge (recall that increases of light intensity are recorded as dark areas in the photograph). The compression wave causes a decrease in the intensity of light emitted by the discharge. Waves of stratification also originate from the cathode region. These will be discussed in another section.

If the average energy of the electrons remained constant during the compression, the increased collision frequency (at the higher pressure) would cause an increase of ionization rate and an increase of the light emitted by the discharge. Since the light intensity decreases in the compression phase, the electron energy must decrease. Increased elastic collision or decreased electric field may explain this decrease of electron temperature. These will be examined in a later section.

Figure 3-6 shows anode to cathode propagation of an acoustic wave produced by the pulse discharge. In this figure, the path of the acoustic wave is shown as a bright line preceded by a thin dark line. The bright line indicates a decrease of light intensity in the compression phase, and is caused by a decrease in the electron temperature. The dark line indicates an increase of light intensity at the leading edge of the wave. Two mechanisms can cause this increase:

(a) compression with constant electron temperature (phase lag of temperature change)

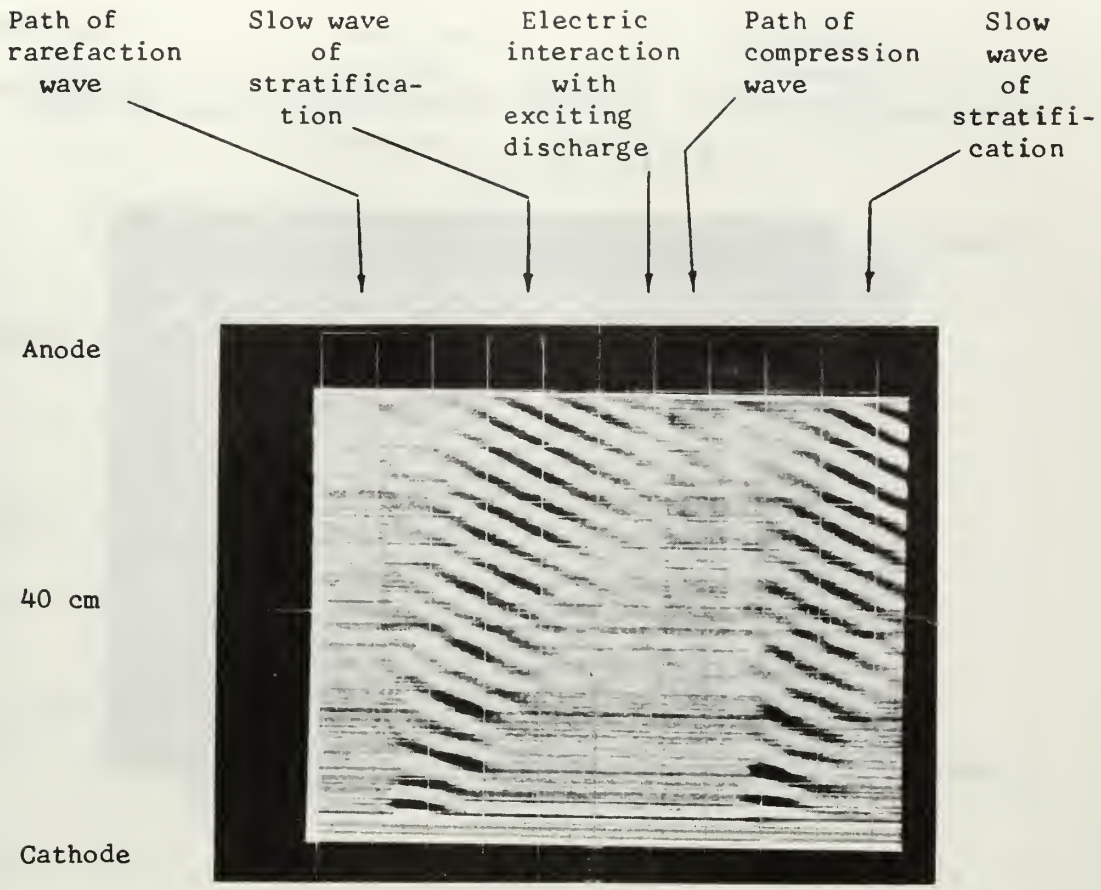

Figure 3-5. Time and space development of light intensity in a 1.3 torr, 2.6 ma neon discharge resulting from anode to cathode propagation of rarefaction and compression waves produced by square wave modulation of the exciting discharge. Lighter areas in photo correspond to darker areas in the discharge. Time scale is 2.0 msec/division.

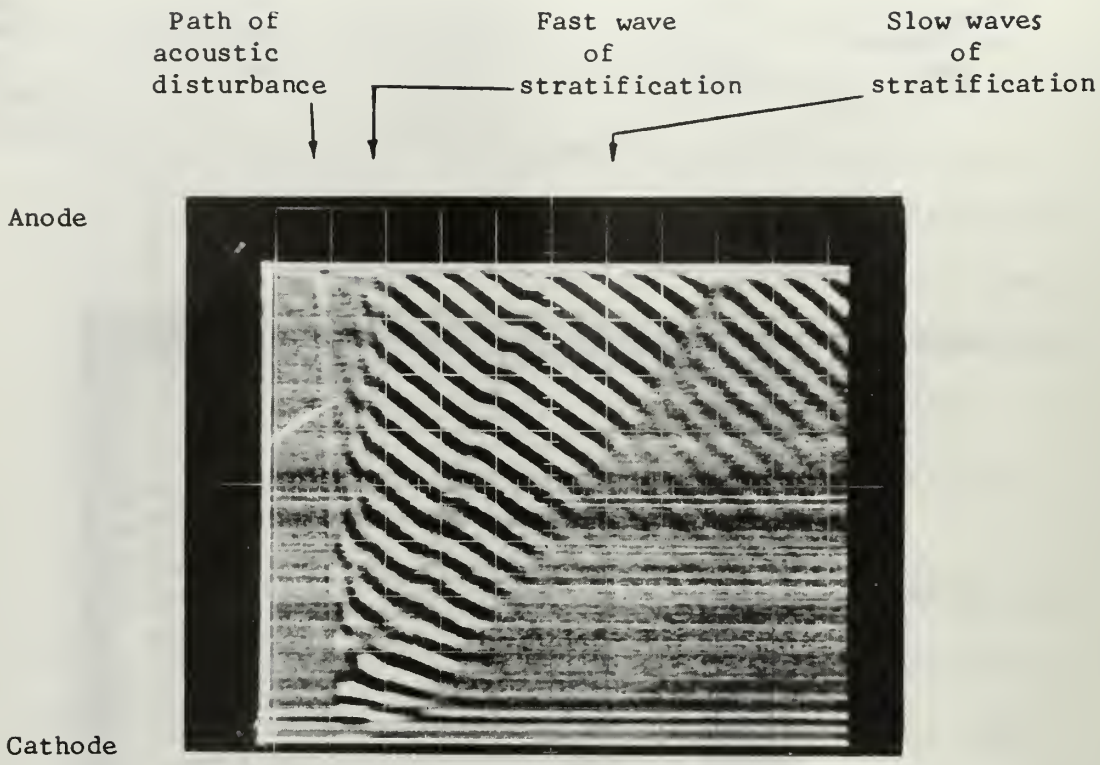

Figure 3-6. Time-space development of light intensity in a 2.2 torr neon discharge at 3.1 ma. Anode to cathode propagation of a compressive acoustic disturbance. Time scale is 2 msec/division. Thin dark line preceding bright line in acoustic interaction indicates a slight increase of ionization rate.

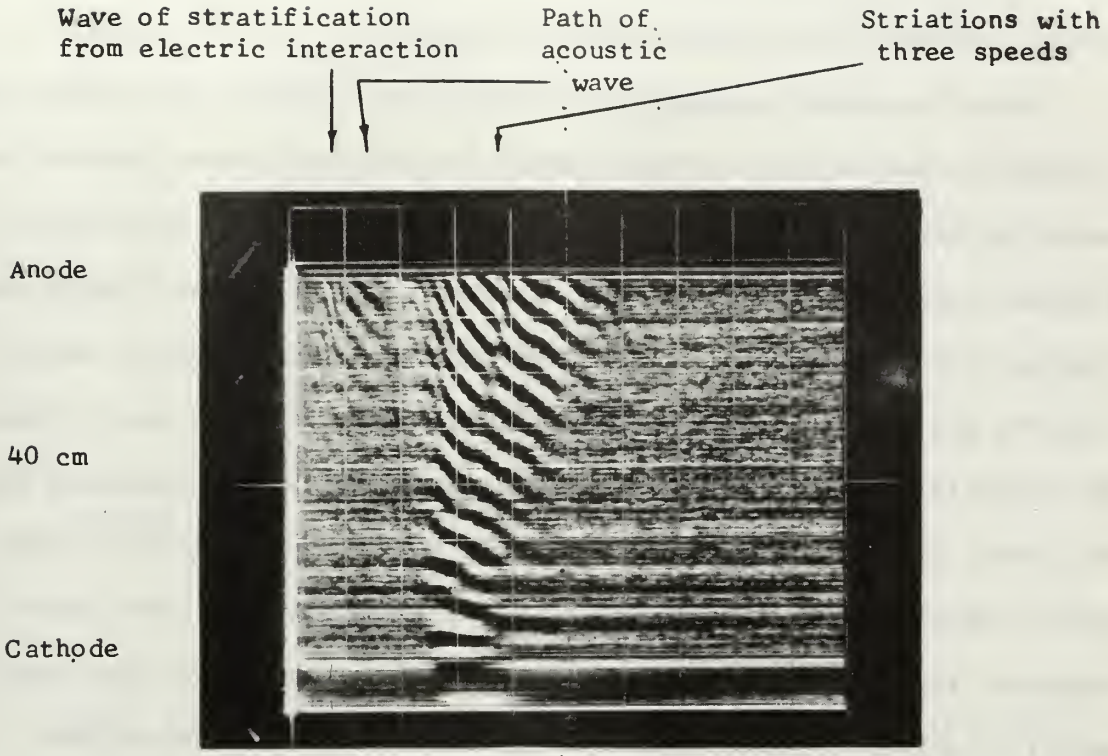

Figure 3-7. Time-space development of light intensity in a 0.82 torr 35 ma neon discharge. Anode to cathode sound propagation. Time scale 1 msec/division. Striation speeds are 140m/sec, 66 m/sec, 33 m/sec respectively. The fastest striations appear to be excited by travel of the acoustic wave along the positive column.

(b) increase of electric field and electron temperature.

This phenomenon was not observed in all photographs with the high-voltage pulser, and was never seen when square wave modulation of the discharge current was used for acoustic wave production.

Anode to cathode propagation of the acoustic wave causes changes of ionization rate in time and space which are similar to those present in moving striations. Figure 3-7 shows striations which are apparently produced during propagation of the acoustic waves along the column. By viewing this photograph along the apparent path of the acoustic wave, with the eye near the plane of the page, a series of lines can be seen. The acoustic wave arrives at the anode 1.6 msec after the beginning of the sweep. At this time, light intensity is observed to increase (dark area in photograph). This increase can be followed, with some interruptions, for most of the distance of the column. A second dark area parallel to this is also visible at the anode end of the photograph. The position at which the third dark line should appear is somewhat obscured by the bright areas associated with the maximum density portion of the acoustic wave. Succeeding striation patterns become clearer.

Striation production by the acoustic waves in an inhomogeneous positive column is considered in the following section.

C. Interaction in an Inhomogeneous Positive Column

As the acoustic wave encounters standing striations in the positive column, changes of the ionization rate at these points also produce moving striations. Light intensity gradients are small for all but the first few standing striations, so that translation of the gas will produce negligible variation of the photomultipler signal in that half of the positive column toward the anode. Figure 3-8 shows the standing

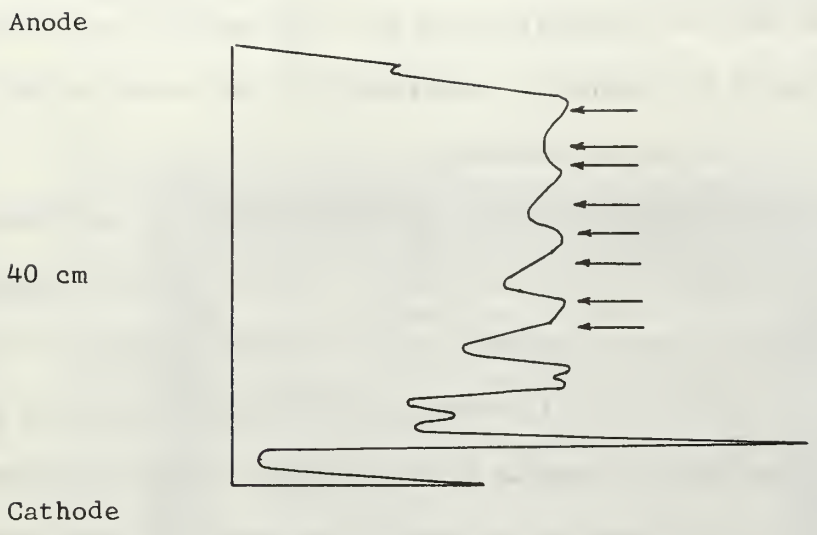

Figure 3-8. Light intensity as a function of position in a 0.82 torr, 15 ma neon discharge. Standing striation patterns had similar form at 10 ma, smaller amplitudes. Arrows show approximate phases of standing striations at which moving striations of figure 3-9 originate. (Small variation as light decreases to zero at anode end is due to a layer of sputtered material on the glass.)

striation configuration in a 15 ma discharge at a pressure of 0.82 torr. Figure 3-9 shows the production of moving striations by the acoustic wave as it encounters the standing striations. These decay and merge directly into the wave of stratification which is excited from the standing striations nearer the cathode. Wavelength of the standing striations is twice that of the moving striations.

Amplification of the wave of stratification increases as discharge current is brought near a critical current (at which self-excited striations occur). Waves of stratification can be excited by smaller localized changes of ionization rate in these cases. Figure 3-6 shows production of a fast and a slow wave of stratification from the region near the second standing striation, and a second slow wave from the cathode region. In both cases it is difficult to fix the point of origin of the wave. A third slow wave is visible at the right hand side of the photograph. This is due to oscillation of tube voltage and current as the first two slow waves arrive in the anode region. Figure 3-7 also shows waves of stratification originating from more than one region of the discharge.

At lower currents, amplitude of the standing striations is smaller, and waves of stratification originate only in the cathode region. Figure 3-5 shows that waves of stratification originating in the cathode region due to compression and rarefaction acoustic waves have nearly opposite courses of development of light intensity. The change of electric field in the cathode region causes the wave of stratification to be excited. Since the compression and rarefaction waves have opposite effects on both of these quantities, the waves of stratification which are produced should be opposite in their course. Theory and experiment have shown that the

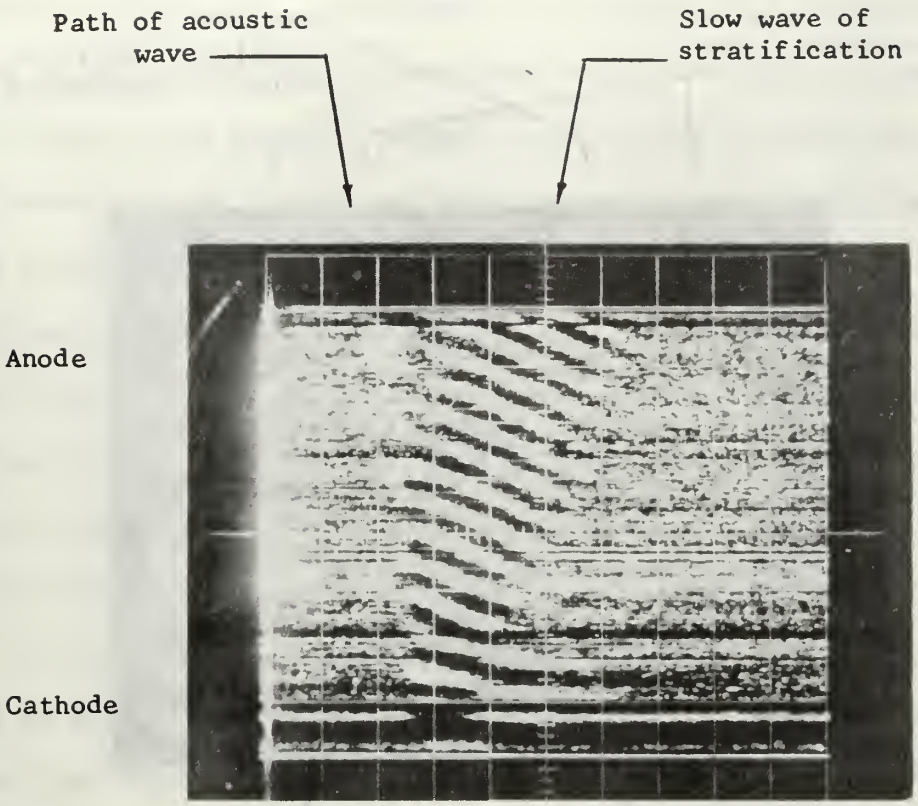

Figure 3-9. Time-space development of light intensity in a 0.82 torr, 10 ma discharge. Anode to cathode propagation of the acoustic wave. Time scale is 1 msec/division. Striation production by sound wave is evident.

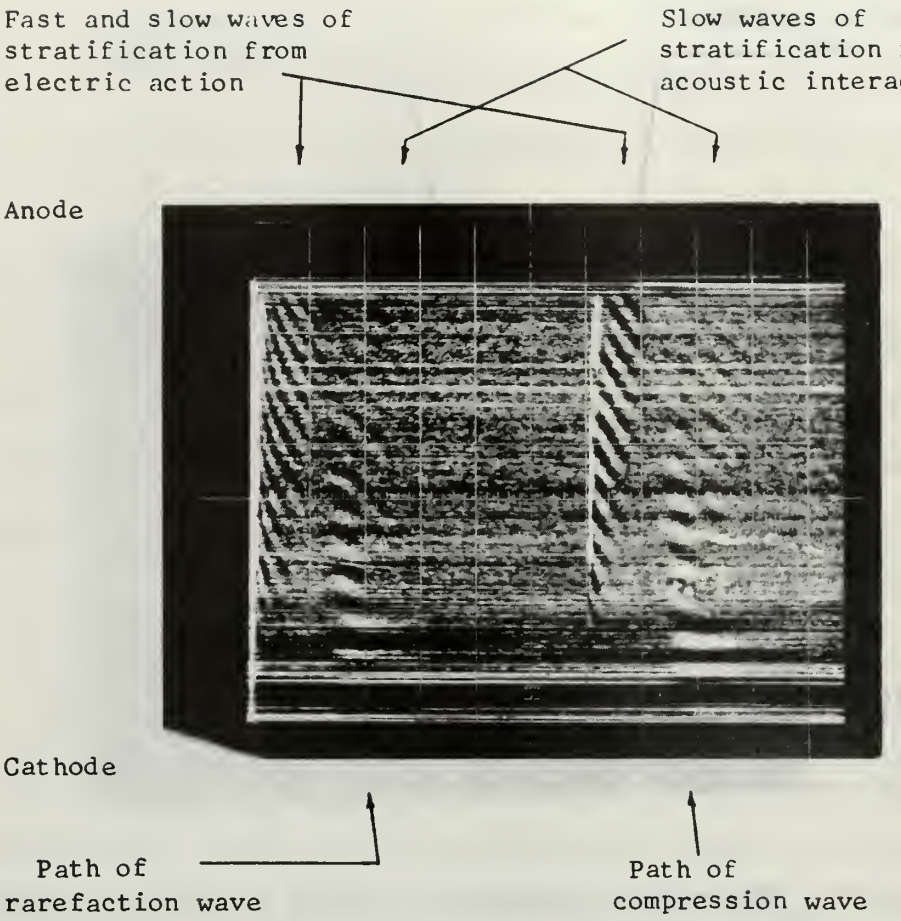

Figure 3-10. Time-space development of light intensity in a 0.7 torr 16 ma neon discharge. Anode to cathode propagation of acoustic disturbances. Time scale is 2 msec/division.

wave of stratification is an "odd" (signed) effect. [43, 48]

The effect of direction of propagation is illustrated by comparing figures 3-10 and 3-11. In figure 3-10, the wave of stratification produced in the cathode region following anode to cathode propagation of the acoustic wave is highly damped. For cathode to anode propagation of the acoustic wave, striations appear along its path. This behavior was also noted in a 4.0 torr discharge, where striations associated with the fast wave of stratification were excited along the path of the acoustic wave (figure 3-12). Group velocity of the wave of stratification is 160 m/sec, significantly smaller than the sonic velocity, and the striations excited by the acoustic wave are attenuated before being amplified again in the wave of stratification.

In figure 3-13, the acoustic wave is shown to decrease the amplitude of self-excited fast striations. These striations are associated with direct ionization of the neutral gas molecules, and the decrease of electron temperature caused by the acoustic wave reduces the amplitude of the striations.

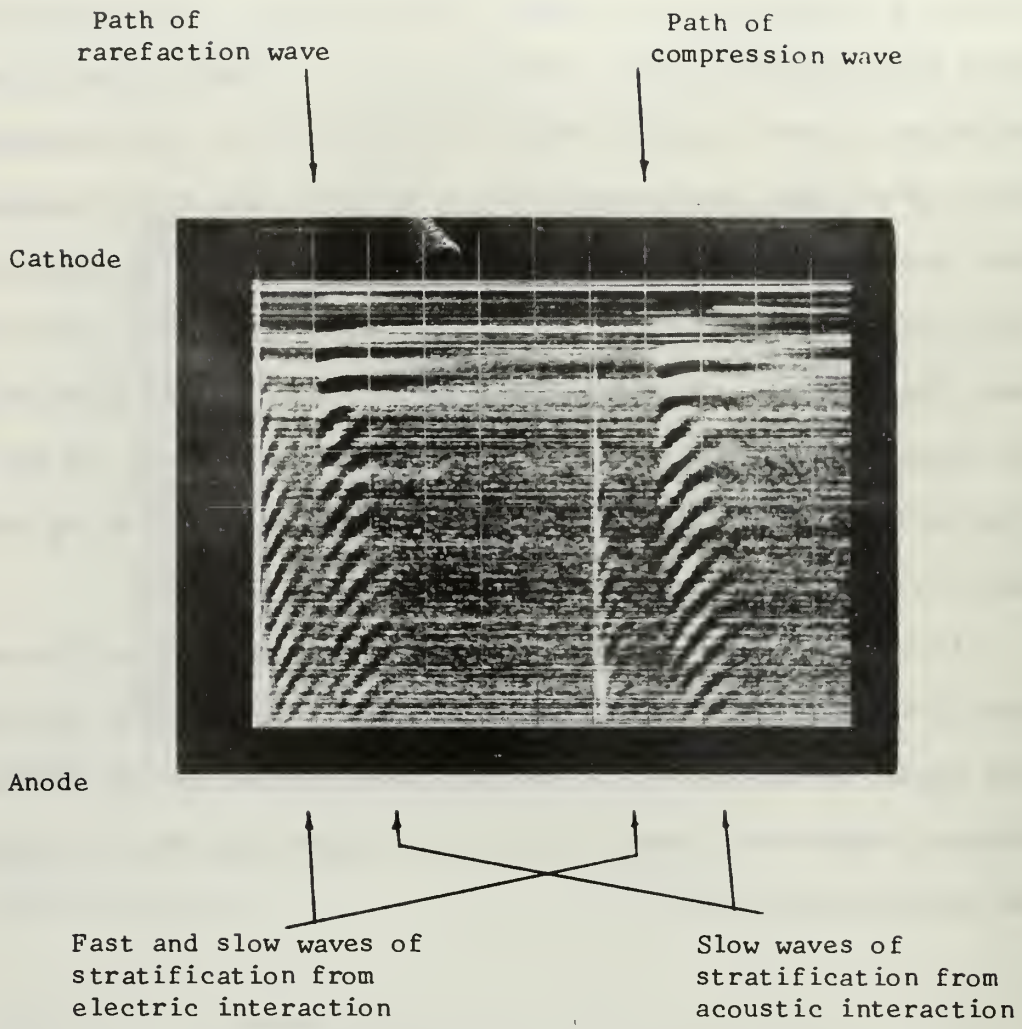

Figure 3-11. Time-space development of light intensity in a 0.7 torr, 16 ma neon discharge. Cathode to anode propagation of acoustic disturbance. Time scale is 2 msec/division.

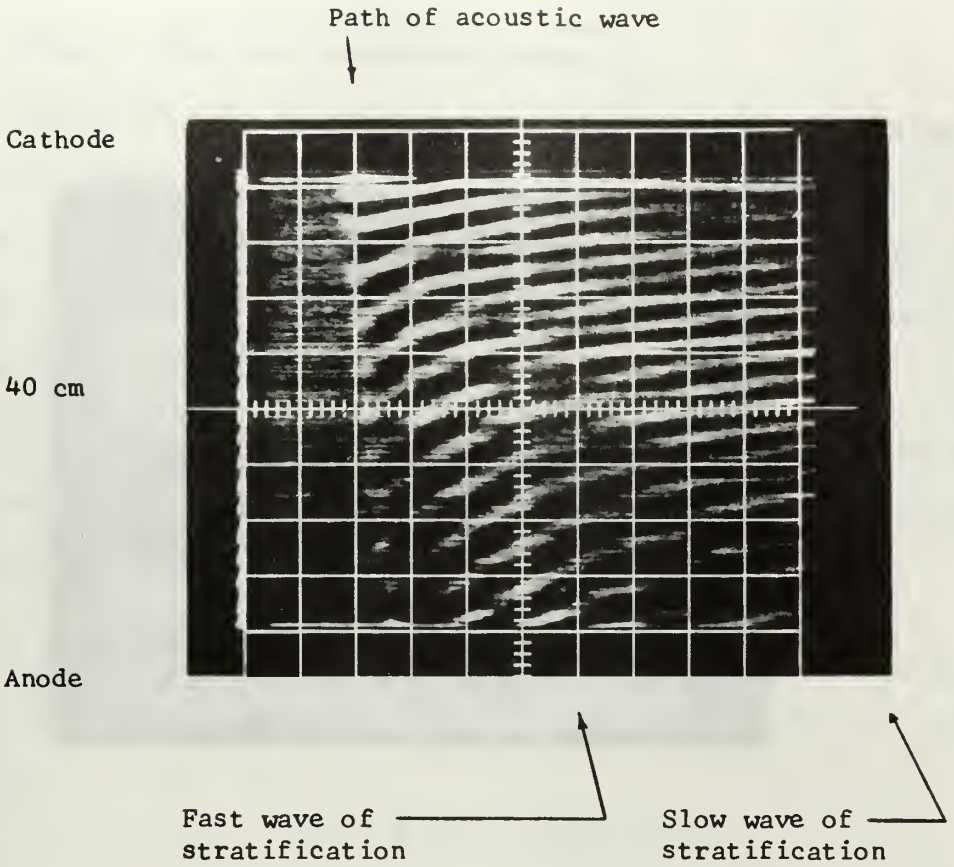

Figure 3-12. Time-space development of light intensity in a 4.0 torr, 0.2 ma neon discharge. Cathode to anode sound propagation. Time scale: 1 msec/division.

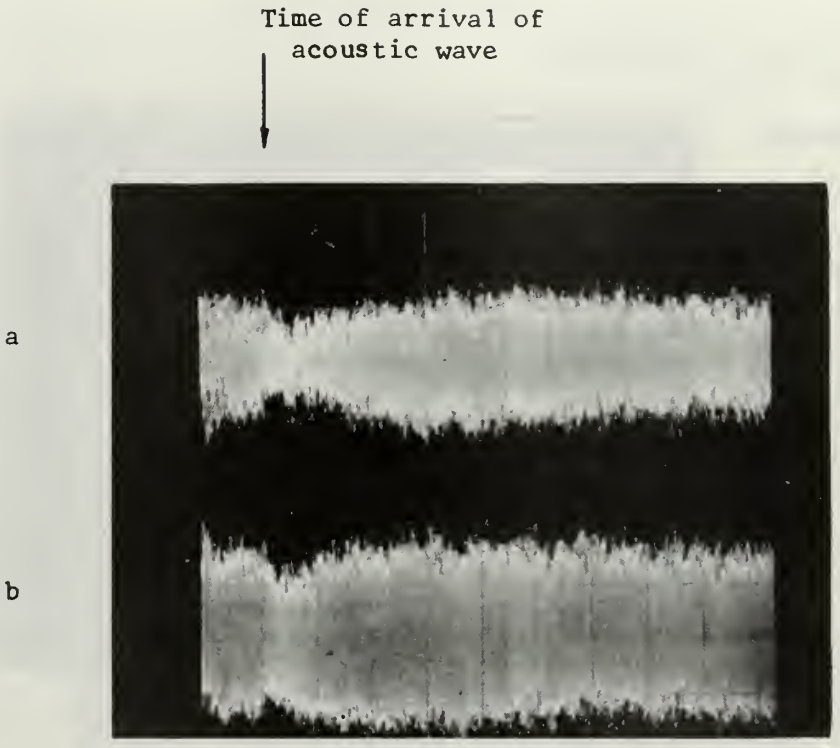

Figure 3-13. Light intensity variation with time at a distance of 1.3 cm in front of the anode. Discharge currents (a) 2.2 ma (b) 2.1 ma; pressure 0.77 torr. Cathode to anode sound propagation. Time scale 2 msec/division, light intensity traces to the same relative scale. Light intensity decreases as compressive acoustic wave arrives.

CHAPTER IV

ANALYSIS OF ACOUSTIC INTERACTIONS IN THE DISCHARGE

A. Change of Electron Temperature

The experiments showed that the light emitted by the homogeneous positive column decreases during the compression phase of the acoustic wave, and that this must be explained on the basis of a change in temperature. In some cases the light emitted by the column increases for a short time preceding this decrease.

Since the ions are nearly in thermal equilibrium with the neutral gas, neutral gas density perturbations will tend to produce the same fractional changes in ion density. These can be expressed as

$$n_+ = \frac{N_{+o}}{N_{no}} \cdot n_n \tag{11}$$

where

$$n_j = N_j - N_{jo} \quad |n_j| \ll N_{jo} \, . \tag{12}$$

Frequencies of the acoustic waves were $\sim 10^3$ Hz, giving a characteristic time of $\sim 10^{-3}$ sec for the ion density perturbation. Ambipolar diffusion times are of the order of

$$\tau_a \approx \frac{R^2}{D_a} = 4 \times 10^{-5} \text{ sec} \, , \tag{13}$$

indicating that ion density changes will be removed through ambipolar diffusion to the walls. However, Saxton observed ion density variations of the form given by equation (11). Diffusion of the charged particle density perturbation evidently does not take place.

The increase of neutral particle density also decreases the mobility of the charged particles, and increases electron energy losses due

to an increase of the collision rate. These tend to bring about a decrease in electron temperature. Electric field may also be varied by the density change, and thus lead to an additional change in electron temperature. In most cases, electron temperature is related to the reduced electric field (E/p), so that it is difficult to separate the effect of field and pressure variations on the electron temperature for this experiment.

Using the relation between electron temperature, pressure (density) and electric field given in [17], it is possible to examine the effects of neutral gas density variations. This equation is

$$T_e = \frac{\sqrt{2}}{3} \frac{\lambda_e}{\sqrt{f_-}} \cdot E \qquad (14)$$

where

T_e is in eV

λ_e electronic mean free path

$= 1/\sigma \cdot N_n$

f_- fraction of electron energy lost per collision.

This equation can be written

$$T_e = \frac{\sqrt{2}}{3 \cdot \sigma} \cdot \frac{1}{\sqrt{f_-}} \cdot \frac{E}{N_n} \qquad (15)$$

Von Engel graphs the variation of f_- as a function of E/p in [17]. The curve is for a constant neutral gas temperature and is therefore equivalent to f_- as a function of E/N_n. For pressures and fields in the experimental range this dependence can be expressed as

$$f_- = f_{-o} \left(\frac{E}{p}\right)^b . \qquad (16)$$

Variation of electron temperature with neutral gas density can therefore

be determined from

$$\frac{\partial T_e}{\partial N_n} = \frac{\partial T_e}{\partial (E/p)} \cdot \frac{\partial (E/p)}{\partial N_n} \quad . \tag{17}$$

In general

$$\frac{\partial T_e}{\partial (E/p)} = \frac{2}{3\sqrt{2}\,\sigma} \frac{1}{\sqrt{f_-}} \left[1 - \frac{b}{2} \right], \tag{18}$$

and

$$\frac{\partial (E/p)}{\partial N_n} \simeq \frac{1}{p} \left[\frac{\partial E}{\partial N_n} - \frac{E}{N_n} \right] \tag{19}$$

so

$$\frac{\partial T_e}{\partial N_n} = \frac{T_e}{E} \left[1 - \frac{b}{2} \right] \cdot \left[\frac{E}{N_n} - \frac{E}{N_n} \right]. \tag{20}$$

In the succeeding paragraphs, it will be shown that $\partial E/\partial N_n \leq 0$. With this knowledge, the temperature change with density depends upon b as follows

$$b < 2 \qquad \frac{\partial T_e}{\partial N_n} < 0$$

$$b = 2 \qquad \frac{\partial T_e}{\partial N_n} = 0$$

$$b > 2 \qquad \frac{\partial T_e}{\partial N_n} > 0 \ .$$

For the case of neon in the experimental range of reduced field (0.8 - 5.0 v/cm · torr), b = 1.9. Thus the variation of electron temperature with pressure is small.

Electric field variation can be analyzed on the basis of the work of Pekarek and Masek. [58] In their method, the electron density variation is assumed to follow the ion density variation quasi-statically, with its form governed by the continuity equation:

$$\frac{\partial N}{\partial t} + \nabla \cdot (N\vec{V}) = Q. \tag{21}$$

When perturbations of the form

$$n_- = N_- - N_{-o} \qquad |n_-| \ll N_{-o} \tag{22}$$

$$e = E - E_o \qquad |e| \ll E_o \tag{23}$$

are substituted, this equation becomes

$$0 = D_- \frac{\partial^2 n_-}{\partial z^2} + \mu_- E_o \frac{\partial n_-}{\partial z} + \mu_- N_o \frac{\partial e}{\partial z}$$

$$+ N_o E_o \frac{\partial \mu_-}{\partial N} \cdot \frac{\partial n}{\partial z} . \tag{24}$$

Electric field is related to charged particle density through Poisson's equation

$$\frac{\partial e}{\partial z} = \frac{q_o}{4\pi \epsilon_o} (n_+ - n_-) . \tag{25}$$

Since

$$\mu_- = \frac{k'}{N_n} , \tag{26}$$

then

$$\frac{\partial \mu_-}{\partial N_n} = -\frac{\mu_-}{N_n} \tag{27}$$

and equation (24) can be written in the form

$$D_- \frac{\partial^2 n_-}{\partial z^2} + \mu_- N_o \frac{\partial e}{\partial z} = 0. \tag{28}$$

Using the two-sided Laplace transform defined in [61] by

$$f(s) = s \int_{-\infty}^{\infty} h(t)\, e^{-st} dt , \tag{29}$$

the equation for the electric field is

$$\bar{e} = \frac{1}{s} \frac{q_o}{4\pi\epsilon_o} \left[1 - \frac{1}{1 - \lambda_D^2 s^2} \right] \tag{30}$$

where $\bar{e}$ is the operator image of e. Equation (30) is to be compared with Pekarek and Masek's equation (10) which is

$$\bar{e} = \frac{1}{s} \left(\frac{q_o}{4\pi\epsilon_o} \right) \left[1 - \frac{1}{1 - 2\left(\frac{\lambda_D}{\ell_1}\right)\lambda_D s - (\lambda_D s)^2} \right] \tag{31}$$

where $\ell_1 = 2D_- / \mu_- E_o$. (32)

The acoustic perturbation therefore gives a result similar to letting $\ell_1 \to \infty$, for which the change of electric field is zero.

If the change of mobility is not taken into account, the compressive acoustic perturbation can be handled through their calculation for $\ell_1 = 100\ \lambda_D$. This causes an electric field change of -2.5×10^{-3} v/cm for a fractional density variation of 0.5 per cent.

Comparing the terms in the last bracket of equation (20), and assuming $E_o = 2$ v/cm

$$N_n = 3.5 \times 10^{16}\ \text{cm}^{-3},$$

we find

$$\frac{\Delta E}{\Delta N_n} = -1.3 \times 10^{-17}$$

$$\frac{E}{N_n} = 5.7 \times 10^{-17}\ .$$

Thus the terms are of the same order of magnitude. It has been assumed that the perturbation of ion density does not decay due to ambipolar diffusion to the walls. If ambipolar diffusion does prevent this field change, there is still a temperature variation resulting from the neutral gas density perturbation. Such a change must be attributed to

variation of collision losses as the collision frequency is changed.

Magnitude of the temperature change can be obtained from equation (20). Recasting it in the form

$$\frac{\Delta T_e}{T_e} = \left[1 - \frac{b}{2}\right] \cdot \left[\frac{\Delta E}{E} - \frac{\Delta N_n}{N_n}\right], \tag{33}$$

the effects of fractional changes of electric field and neutral particle density are readily seen. For the conditions given in the preceding paragraph

$$\frac{\Delta T_e}{T_e} = -9.3 \times 10^{-4} . \tag{34}$$

The predicted temperature variation is therefore of the order of one part in 10^3. Sensitivity of the time space display method is quite evident from this value.

The short duration increase of light intensity which sometimes preceded the longer decrease in the compression phase may be due to the effect of the finite length of the acoustic waves. This finite length wave can be described by

$$\xi = -\xi_o \sin(kZ - \omega t)\, U(t - \frac{Z}{c}) \tag{35}$$

for a wave which is propagating from anode to cathode with velocity c, and a compression phase at the leading edge. In this equation

$$\xi = N_n - N_{no} , \quad |\xi| << N_{no} \tag{36}$$

and the wave is of semi-infinite extent. An exponential damping term should be included to give a form similar to that shown in figure 2-5.

The change of ionization rate can be expressed as

$$\frac{dz}{dt} = \frac{dz}{dN_n} \cdot \frac{dN_n}{dt} \tag{37}$$

and from [17]

$$\frac{dz}{dN_n} = - c_1 x^{3/2} e^{-x} \tag{38}$$

where

$$x = eV_i/kT_e$$

Thus

$$\frac{dz}{dt} = c_1 \xi_o x^{3/2} e^{-x} \left[- \omega \cos(kZ - \omega t)\ U(t - \frac{Z}{v}) \right.$$

$$\left. + \sin (kZ - \omega t) \cdot \delta(t - \frac{Z}{v}) \right], \tag{39}$$

and the solution will have a transient which propagates. This transient may explain the slight increase of ionization rate sometimes observed at the leading edge of the acoustic wave.

B. Excitation of Acoustic Waves by the Discharge

Ingard has predicted that acoustic waves can be generated in the neutral gas of a discharge through collisions with the charged particles. [27] Working from the linearized equations for continuity of mass, momentum and energy of the neutral gas, with charged particle interactions entering as source terms, he obtains the equation

$$\frac{1}{c^2} \frac{\partial^2 p}{\partial t^2} - \nabla^2 p = \frac{\gamma - 1}{c^2} \frac{\partial H}{\partial t} - \nabla \cdot \vec{F} . \tag{40}$$

In this equation

c	sonic velocity	
	$= \sqrt{\gamma kT_n/M_n}$	(41)
p	variation in pressure	
γ	ratio of specific heats	
H	heat energy source term	
$\vec{F}$	momentum transfer source term.	

This equation shows that acoustic waves can be excited by a change of the heat transfer rate or a spatial gradient in momemtum transfer. Ingard attributed acoustic disturbances from moving striations to the former, while Briand and Delcroix observed acoustic waves which they ascribed to momentum transfer from the ions to the neutral gas. [7]

Before carrying out a calculation to compare the magnitudes of these two effects in the positive column when moving striations are present, it should be pointed out that variation of the power dissipated in the cathode fall due to a change of current will cause a much larger acoustic wave than any change in the conditions of the positive column. Normal cathode fall for neon with a molybdenum electrode is approximately 110 volts; [17] the cathode properties of molybdenum and tantalum are similar. Potential difference between the first two standing striations in the neon positive column is 18.5 volts. [16] This is larger than the potential difference between peaks of moving striations. Assuming all energy dissipated in each region is consumed in gas heating, a stepwise change in discharge current will cause an acoustic wave to originate from the cathode region which will be larger by a factor of 5 than that which will be produced from the region between the standing striations. However, it is possible to have moving striations present in the discharge with no variation in discharge current, or to have current variation small enough that the acoustic waves produced in the cathode region are smaller than those which arise from the moving striations. [10, 11]

Consider the case of acoustic waves produced by perturbations of an infinite, homogeneous dc discharge column. In order to compare the magnitudes of the source terms in the equation derived by Ingard, it is

assumed that the electric field is 2.0 volts/cm, electron temperature is 2.0 eV, and neutral gas pressure is 1.1 torr. Under these conditions, the following parameters are applicable [17]

$$N_- = 2.4 \times 10^{16}\ m^{-3}$$

$$\mu_+ = 1.2\ m^2/\text{volt sec}$$

$$\mu_- = 80\ m^2/\text{volt sec}$$

$$\lambda_+ = 1.2 \times 10^{-4}\ m$$

$$\lambda_- = 6.6 \times 10^{-4}\ m\ .$$

As an approximation to the momentum transfer term, it can be assumed that all momentum gained by a charged particle from the electric field in traveling one mean free path along the direction of the electric field is given to a neutral particle at the end of that free path. This corresponds to the fact that distribution functions of charged particles in electric fields can be divided into a part which is symmetric (isotropic) and a part which is asymmetric. The average energy of the symmetric part is much larger, and for electrons, corresponds to the temperature measurable by an electric probe. Average velocity of the asymmetric part corresponds to the mobility or drift velocity. Assuming that all particles have the drift velocity of the particular species, the momentum transfer is given by

$$\vec{F} = n(m_+ \cdot \vec{v}_+ \cdot \nu_{c_+} + m_- \cdot \vec{v}_- \cdot \nu_{c_-}). \qquad (43)$$

The effective collision frequency for asymmetric momentum transfer is

$$\nu_{c_\pm} = |v_\pm| / \lambda_\pm\ , \qquad (44)$$

and as the elastic collision cross-section of neon is nearly independent of energy, the mean free path is essentially constant. The velocities

used in calculating these collision frequencies are mobility velocities

$$\vec{v}_{\pm} = \pm \mu_{\pm} E \tag{45}$$

since only collisions along the direction of drift motion are to be considered for momentum transfer. This gives

$$\vec{F} = n\left(\frac{m_+ \mu_+^2}{\lambda_+} - \frac{m_- \mu_-^2}{\lambda_-}\right) \vec{E} \cdot \left|\vec{E}\right| \tag{46}$$

Comparison of the magnitudes of ion and electron contributions to this equation shows that

$$\frac{m_+ \cdot \mu_+^2 \cdot \lambda_-}{m_- \cdot \mu_-^2 \cdot \lambda_+} \approx 45, \tag{47}$$

and the electrons can be neglected. Note that this is independent of electron and ion temperature. Thus the equation of interest is

$$\nabla \cdot \vec{F} = 2 \cdot n \cdot \frac{m_+ \mu_+^2}{\lambda_+} \cdot |E| \cdot \frac{\Delta E}{\Delta x} . \tag{48}$$

Large changes of electric field are observed in the presence of moving striations, and an assumption of

$$\frac{\Delta E}{\Delta x} = 1 \text{ volt/cm}^2$$

is well within the range found in other experiments. [12, 67] With these values,

$$\nabla \cdot \vec{F} = 38.4 \text{ joules/m}^5 \tag{49}$$

To compare this with the heat energy term resulting from the change of electron temperature in moving striations, it is assumed that electron temperature is doubled in 20 microseconds, that each electron has the energy of the distribution function average and that all electrons collide elastically with neutral atoms. The fraction of energy given up

by each species in an elastic collision is denoted $f_{\pm}$. Relative contributions of ions and electrons can be approximated by

$$\frac{H_-}{H_+} = \frac{n_- \cdot f_- \cdot \nu_{c-} \cdot kT_-}{n_+ \cdot f_+ \cdot \nu_{c+} \cdot kT_+} = 26. \qquad (50)$$

Thus the ion contribution can be neglected, especially since the temperature of the electrons doubles while that of the ions changes little.

Ingard gives the following equation to express the heat contribution of the electrons [27]

$$\frac{\gamma-1}{c^2}\frac{\partial H}{\partial t} = P_o\left[\left(\frac{m_e}{m_n}\right)^{\frac{1}{2}}\frac{1}{c}\frac{\partial}{\partial t}\left[\left(\frac{T_e}{T_n}\right)^{3/2} N_e \langle\sigma'\rangle\right]\right]. \qquad (51)$$

Assuming the temperature change to be the dominant factor, this equation becomes

$$\frac{\gamma-1}{c^2}\frac{\partial H}{\partial t} = P_o\left[\left(\frac{m_e}{m_n}\right)^{\frac{1}{2}}\frac{1}{c}\frac{3}{2}\frac{N_e}{T_n^{3/2}}\langle\sigma'\rangle\right] T_e^{\frac{1}{2}}\frac{\partial T_e}{\partial t} \qquad (52)$$

where

$$\langle\sigma'\rangle = 6 \cdot (\gamma - 1)\left(\frac{3}{\gamma}\right)^{\frac{1}{2}}\langle\sigma\rangle = 5.2\ \langle\sigma\rangle$$

$$\langle\sigma\rangle = 3.95 \times 10^{-20}\ m^2$$

$$N_e = 2.4 \times 10^{16}\ m^{-3}$$

$$c = 456\ m/sec$$

$$T_n = 300\ ^oK.$$

Using the values, and the postulated temperature change,

$$\frac{\gamma-1}{c^2}\frac{\partial H}{\partial t} = 3.52 \times 10^2\ joules/m^5. \qquad (53)$$

This is an order of magnitude larger than the contribution from the momentum term. Discharge conditions under which E, $\frac{\Delta E}{\Delta x}$ and Δt are larger and ΔT_e is smaller, will change these comparative magnitudes.

The experiment of Briand and Delcroix was performed with a plasma produced by an rf discharge. The voltage between two grids bounding this plasma was varied at a given frequency, and a microphone located normal to the plane of these grids. Acoustic waves were detected at the frequency of this modulating voltage. Since the rate of heat generation is unchanged by the small modulation signal, these acoustic waves must be generated by the term $\nabla \cdot \vec{F}$, i.e., a net transfer of momentum to the neutral gas by the ions. Amplitude of these waves was observed to increase as the R-F power increased. Charged particle density increases as this power increases, and as $\nabla \cdot \vec{F}$ is linearly dependent upon this density, the experiment and theory are in agreement.

APPENDIX I

DISCHARGE PROCESSES

This appendix is included for the reader who is unfamiliar with glow discharges. The discharge is described generally, and then discussed from a microphysical point of view. Particular attention is paid to processes important to wave of stratification theory. Cobine [13], von Engel [17] and Loeb [37] all treat the discharge processes in more detail, and the stratification work has recently been reviewed by Oleson and Cooper [40].

A. General Description

Figure 4-1 shows schematically the major areas of a low-pressure, cold cathode dc glow discharge. A discharge of this type in any vessel has a cathode fall of definite length determined by the gas pressure and type, and by the electrode material. This region is essential to the production of electrons for the discharge. The positive column is the next important region. A glow discharge can be operated without a positive column. Whenever the discharge is longer than the cathode fall, the positive column fills the remaining space between the negative glow and the anode. It is this part of the discharge which is used for plasma research when a weakly ionized medium is suitable. Commercial applications of the positive column use its light output in "neon" signs and fluorescent lights. The anode fall region produces ions for the positive column, and is not important unless this fall of potential becomes unstable. In this case, anode spot oscillations develop and disturb the properties of the positive column.

Current in the discharge can be varied over more than three decades (0.5 to 500 mA) with constant voltage drop across the discharge tube.

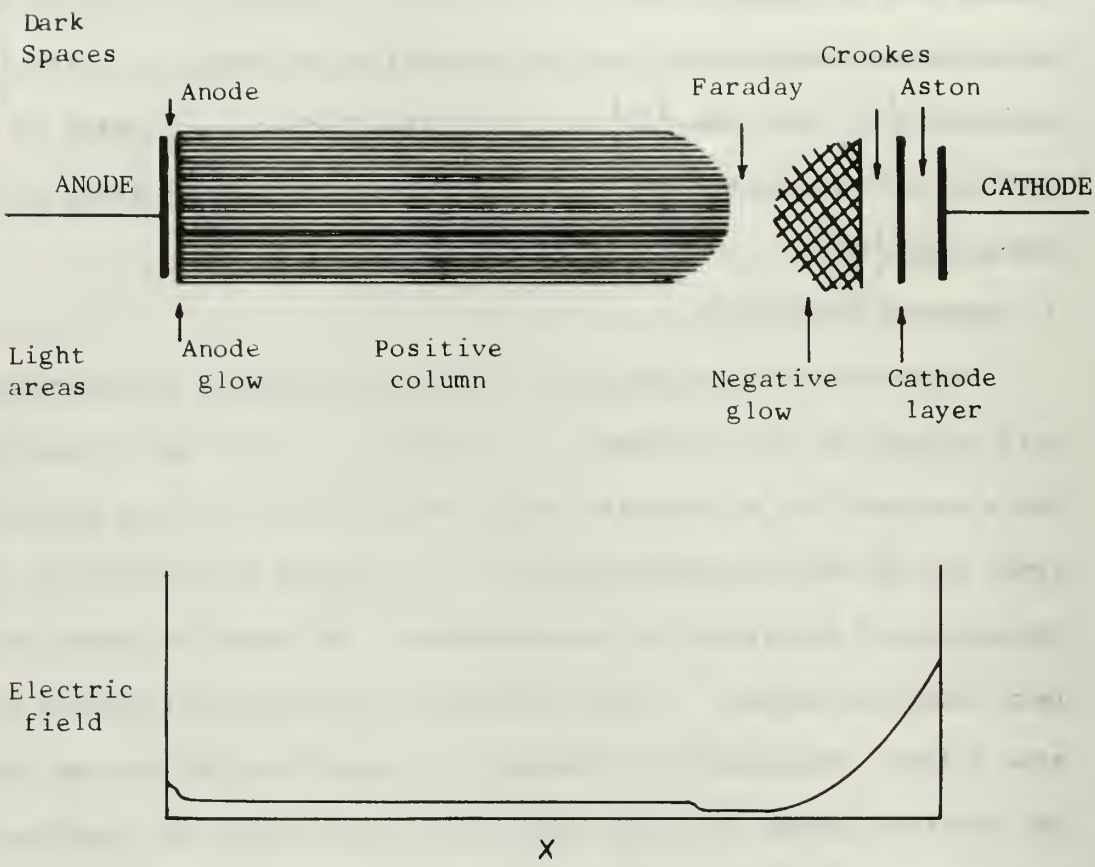

Figure 4-1. Characteristic light and dark areas of a low pressure dc glow discharge. Lower sketch shows electric field as a function of position in the positive column, with the coordinate system chosen such that the positive X direction is in the direction of the electric field.

This current-voltage behavior characterizes the normal glow regime, and finds application in voltage regulator tubes. For discharge currents of several hundred milliamperes, heating of a cylindrical cathode becomes noticeable. Heating of the tube walls also becomes appreciable at these higher currents, particularly in narrow tubes. Sputtering of cathode material onto the walls of the discharge tube presents a problem, however, particularly as pressure is reduced below two torr.

The light emitted by each section of the discharge is characteristic of that region, and increases with increasing discharge current. Light from the negative glow in neon is always orange, as is that from the anode fall when this is visible. In the positive column, a definite change of color from orange to red is observed as either current or pressure is increased. A standing striation always heads the positive column, and several other spherically-shaped light regions can be observed in the column at lower pressures within the experimental range. These are highly damped toward the anode. Viewing the striations with a prism spectrograph shows that lower energy (red) lines are excited closest to the cathode with orange and green lines appearing toward the anode.

Thermionic emission of the electrons from a heated tungsten wire or heated oxide-coated cathode eliminates the cathode fall region. Other surfaces will produce electrons without heating and allow a low potential difference to be used in maintaining the discharge. [24] Cold cathode operation was chosen for these experiments for several reasons: (1) no external power supply is needed as in the case of the heated cathodes; (2) electrodes may be identically constructed and the polarity reversed to check for any directional dependence in the tube; (3) simplicity of

construction; (4) insensitivity of this cathode to any environment as opposed to the oxide coated cathodes.

Regardless of choice of cathode, the negative glow is always present and it is this glow that gives the discharge its name. Approximately equal numbers of positive and negative charges are present, making this the first region with plasma characteristics.

The plasma of the positive column is a slightly ionized gas, with fraction of ionization 10^{-6} to 10^{-4}. Collisions with neutral atoms play a dominant role in this region. Mobility and ambipolar diffusion (described later) govern the motion of charged particles in the column, and recombination is assumed to be significant only at the walls. A small positive gradient of potential in the direction of anode is essential for the production of the charged particles which maintain the discharge, and it is this positive gradient which names this portion of the discharge.

B. Cathode Fall

Electron production at the cathode is accomplished primarily through acceleration of ions into the metal surface by the high electric field present in this region (figure 4-1). As the ejected electrons are accelerated away from the surface by this same field, they excite neutral atoms and form the cathode layer. Further acceleration raises electron energy above the ionization level and leads to production of more electrons, this time in the Crookes dark space. These electrons repeat this chain of events, and the multiplication process grows exponentially with distance from the cathode.

If we let α denote the number of ionizations per unit length of travel of an electron, and assume that the ionization per length is

proportional to concentration, then a single electron emitted at the cathode will give

$$\exp\left(\int_0^d \alpha \, dx\right) \tag{54}$$

electrons at a distance d from the cathode. Assuming also, that $1/\gamma$ ions must impinge upon the cathode to cause emission of a single electron, in the steady state each electron emitted must create $1/\gamma$ ion pairs to maintain the discharge. Thus

$$\gamma\left[\exp\left(\int_0^d \alpha \, dx\right) - 1\right] = 1 \tag{55}$$

and

$$\int_0^d \alpha \, dx = \ln\left(1 + \frac{1}{\gamma}\right) . \tag{56}$$

The integral gives the number of ionizing collisions from the cathode to d. This can also be approximated by

$$\int_0^d \alpha \, dx = \eta V_n , \tag{57}$$

where η is the number of ion pairs per electron per volt of potential, and V_n is the normal cathode fall:

$$V_n = \frac{1}{\eta} \ln\left(1 + \frac{1}{\gamma}\right). \tag{58}$$

This equation shows that normal cathode fall increases as ionization efficiency decreases, and as the efficiency of production of secondary electrons decreases. For the case of neon gas and an aluminum cathode, the normal cathode fall is 120 volts, and the length of the cathode fall at one torr is 0.64 cm. [16] Tantalum has a slightly lower fall of potential and shorter dark space, as its characteristics are similar to that

of molybdenum. [3] Complete data on tantalum were not available.

Cathode potential fall can be reduced and current density increased by improving the secondary emission coefficient--the term γ in equation (58). Although ions have been mentioned as producing the electrons, ultraviolet photons can also produce electrons through the photoelectric effect. This effect is enhanced by using two large closely-spaced parallel plates as cathodes, and is called the hollow cathode effect. It may also be obtained by using a cylindrical shell of small diameter, and it was in this manner that the hollow cathode effect was used in these experiments. Investigations which have been reported show the importance of separation distance for flat plates, and the variation of this distance with the gas and the pressure. [78, 79] Although no data was available for the cylindrical shells, the flat plate data gave an idea of the minimum and maximum diameters which could be used in the pressure range of these experiments.

Magnetic fields placed such that the magnetic lines are parallel to the plane of the electrodes have been used in conjunction with the hollow cathode construction. [62, 63] These fields have the same effect as increasing pressure, provided certain limits are observed. Since an equivalent pressure increase can be obtained, the effective lower pressure limit for a given geometry can be reduced.

As electrons leave the high field region of the cathode fall, their average energy is reduced. The light emitted in the negative glow shows this, as higher energy spectral lines appear nearest the cathode.

Sputtering of cathode material onto the discharge tube walls hinders observation of cathode area light intensity. It has a much more serious effect in the case of a sealed tube, for the pressure is decreased as gas

molecules are shot into the cathode surface or adsorbed on the surface formed by the sputtered material. Variation of sputtering rate is functionally dependent upon a negative power of the pressure, as both ion velocity and sputtered particle free paths are increased in this case. [3]

Acton and Swift note that this power seems to be approximately -5, and on this basis they derive [3]

$$\frac{dp}{dt} = \frac{-c}{p^5}$$

$$p = (p_o^6 - 6\ ct)^{1/6}$$

A tube losing 5% of its pressure in two hours will lose 20% of its pressure in the next four hours. This effect is known as cleanup and can be employed as a means of purifying the gas in a discharge tube. All elements other than helium have ionization energies which are lower than that of neon, and will therefore be ionized preferentially in any region of the discharge. The ions move to the cathode region under the influence of the electric field, where cleanup takes place, leaving the body gas free of impurities.

Druyvesteyn and Penning note that the Faraday dark space contains a "red aureole" in very pure neon. [16] This is believed to be due to the excitation of metastable atoms which have diffused into this region from the positive column or the negative glow. It was used as a check on purity of the discharge gas in all experiments. A mass spectrometer gives the only certain test of the constituent gases of the discharge, and is impractical for ordinary discharge work.

C. Positive Column

Macroscopic properties of the plasma of the positive column such as

the complex conductivity and the spectrum of the emitted light are determined by the microscopic processes governing thermal equilibrium, ionization, mobility and diffusion. The development of moving striations is dependent upon each of these factors.

In this section, after a brief description of plasma and the Debye length, thermal equilibrium is discussed. Elastic, inelastic and electron-electron interactions are included since each of these is important in determining the electron energy distribution function. The form of this function determines whether ionization will be predominantly direct or stepwise, each case giving rise to moving striations with different characteristics.

The diffusion of charged particles, formation of space charges and the effect of electric field changes upon the temperature of electrons are all processes which have been studied as a result of theoretical papers on moving striations.

1. Plasma

Before proceeding with this description of the discharge, it should be pointed out that the weakly ionized gas of the positive column is a plasma. Irving Langmuir first applied this term to the positive columns of discharges with which he was working in order to convey the idea that positive and negative charge densities were approximately equal. Poisson's equation

$$\nabla \cdot E = 4\pi q_o \left[N_+ - N_- \right] \qquad \text{(esu)} \qquad (59)$$

states that large electric fields will be set up whenever $N_+ \neq N_-$, since the values of $N_\pm$ are of the order of 10^{10} cm^{-3}. The mobility of the charged particles will cause this imbalance to be adjusted. The restoring motion will also cause oscillations, but characteristic frequencies

for oscillations of both ions and electrons are far above the range of this experiment. This internal struggle for neutrality gives rise to a characteristic distance for the decay of an artificially introduced potential such as at a probe or the tube wall. Known as the Debye length or Debye shielding distance, it is given by

$$\lambda_D^2 = \frac{kT_e}{4\pi q_o^2 N_-} \tag{60}$$

where

k = Boltzmann's constant

T_e = electron temperature, degrees Kelvin

n_e = electron density, cm^{-3}

q_o = electronic charge, esu .

It must be added that all extraneous fields are not eliminated, and the plasma does not succeed in eliminating local electric fields at all times. In fact, the question of how the positive column supports a macroscopic polarization such as that which accompanies moving striations is the very question which has perplexed investigators for years. This will be clarified in the section on wave of stratification theory.

2. Thermal Equilibrium

The mechanisms involved in attaining thermal equilibrium are rather complex, since the electric field acts as an energy source for the system, directly affecting both ions and electrons, while these charged particles exchange energy among themselves, with each other and with the neutral gas. Finally, there is a large energy sink for high-energy electrons in the form of inelastic collisions leading to excitation and ionization. Several attempts have been made to treat this problem theoretically, and as each work adds more insight into these

fundamental processes, the important aspects of each are given.

Since the maximum fractional energy which a particle of mass m_2 can lose in an elastic collision with a particle of mass m_1 is $\frac{4m_1m_2}{(m_1 + m_2)^2}$, an electron will lose a small fraction of its energy in colliding elastically with a neutral neon atom - approximately 1/37,000 or 2.7×10^{-5} - while an ion will lose up to 1/2 its energy in colliding with a neutral. This allows the electrons to retain more energy gained from the electric field than the ions. Typical average electron energies are of the order of two electron volts (eV), equivalent to a kinetic temperature of about 23,000 degrees Kelvin. Ions also gain energy from the electric field, but ion temperatures differ little from room temperature due to the efficient transfer of energy to the background gas. Thermal equilibrium does not exist between these three species. The interaction between them and among particles of a single type all contribute to establishing a steady state distribution of particles with respect to energy. The average energy of this distribution is then, of course, the energy associated with the temperature.

The distribution of electrons with respect to energy changes as electric field, elastic collisions, electron-electron interactions, and inelastic collisions with neutrals are taken into consideration. In the field-free case, the equilibrium distribution is a Maxwell-Boltzmann function, with the temperature of each component equal to that of the walls. When an electric field is added with only elastic collisions allowed, and the Coulomb interaction between charged particles is ignored, the distribution function is known as a Druyvestyn distribution. [16] A comparison of these two forms of the distribution function shows that the effect of elastic collisions with the neutrals

$$f(\epsilon) = \frac{2}{\sqrt{\pi}} N_e \left[x^{\frac{1}{2}} e^{-x} dx \right]_{(M-B)} \qquad (61)$$

$$f(\epsilon) = \frac{2}{\Gamma(\frac{3}{4})} N_e \left[x^{\frac{1}{2}} e^{-0.55x^2} dx \right] \qquad (62)$$

(Druyvestyn)

$x = \epsilon/\epsilon_o$

ϵ_o = average electron energy

is to reduce the number of high energy electrons. These high energy electrons are essential to excitation and ionization from the ground state. Thus the Maxwell-Boltzmann function will cause more excitations and ionizations for a given temperature.

Druyvestyn also derived the distribution function for the case in which inelastic collisions are allowed, and Smit's calculations based on this work showed the decrease in high energy electrons which can be expected in helium. [73] This loss is reduced as electric field is increased.

Cahn considered elastic collisions and charged particle interactions. [8] His results showed that an increase of electron density caused a change from the Druyvestyn toward the Maxwellian form of the distribution. A similar result was obtained by Gurevich. [23]

Kagan and Lyagushchenko appear to be the first to include both elastic and inelastic collisions and electron-electron interactions in a calculation of the distribution function. [28] Their result for a pressure of five torr and 200 mA is graphed against the Maxwellian function and shows that the number of particles at energies above 9 electron volts is an order of magnitude smaller than the number for a Maxwellian distribution corresponding to the same average energy. [29]

In each of these cases it is evident that elastic collisions with neutral particles cause the deficiency of high energy particles. Reduction of electric field and electron density both serve to make the distribution function short of high energy electrons. Thus non-Maxwellian electron velocity distributions are expected for pressures and currents in the experimental range, with the departure from the Maxwellian form becoming larger as pressure is increased.

The distribution function of electrons in neon has been measured by Vorob'eva, Kagan and Milenin over the pressure range 0.06 to 1.6 torr. [82] At 0.06 torr and 200 mA, the distribution was essentially Maxwellian. For a pressure of 1.0 torr and 100 mA, the fraction of electrons with energy centered at 17 eV is half that corresponding to a Maxwellian function . This shows the change of the function brought about by a pressure change. Data taken at the same pressure, and 25 mA discharge current, show that the distribution decreases more rapidly with energy than the function obtained at 100 mA. Electron-electron interactions tend to make the distribution function Maxwellian. These interactions are reduced as current is decreased, and this explains the further departure of the electron distribution function from Maxwellian.

3. Ionization and Recombination

Ion pairs are produced in the positive column mainly by inelastic collisions of electrons with neutral atoms which are either in the ground state or in a meta-stable state. Photoionization plays a minor role, as ultraviolet photons with wavelength less than 2400 Å are required for ionization from metastable states, and vacuum ultraviolet photons are required for ionization from the ground state.

The general equation for the rate of ionization by electrons can

be written [31]

$$z = \frac{2k^2T_e^2}{m_e^2}\left[N\int_{u_i}^{\infty} Q_i(u)\cdot uf_o(u)du + \sum_s N_s \int_{u_{s_i}}^{\infty} Q_{s_i}(u)\cdot uf_o(u)du\right]. \qquad (63)$$

The first integral represents direct ionization (from the ground state) while the second represents ionization from excited states. Summation is over all excited states, although only the four states with configuration $2p^5 3s$ have populations which are significant. Two of these are metastable. Other symbols not previously used are

u = dimensionless electron energy (eV/kT_e)

u_i = eV_i/kT_e: V_i is the ionization energy of neon

$Q_i(u)$ = ionization efficiency for electron energy u; approximated by $N\cdot Q_i = 0.055(V - 20.6)$

N_s = density of excited atoms at the level denoted by s

u_{s_i} = $e(V_i - V_s)/kT_e$

$N\cdot Q_{i_s}$ = $\gamma\cdot 0.055(V - V_i - V_s)$; γ is determined experimentally, corresponds to a different cross section for the respective states

N = neutral particle density

The equation for Q_i expresses the fact that ionization cross section of the electrons increases with increasing electron energy. This is true for the energies which electrons can obtain under the conditions of these discharges.

In view of the deficiency of high energy electrons noted in the

previous section, direct ionization would be expected to contribute fewer ion pairs than stepwise ionization. A calculation of the relative importance of the two methods of ionization shows that stepwise ionization provides more ions by three orders of magnitude than direct ionization. [29] Comparison with a Maxwell-Boltzmann distribution shows that the distribution function derived with electron-electron, elastic, and inelastic collisions taken into account produces fewer ions from direct ionization by four orders of magnitude. These results lead the authors to conclude that "the role of direct ionization is negligibly small compared with that of stepwise ionization". [30] This is a conclusion which must be contrasted with experimental findings on moving striation behavior.

The change of light emitted by the discharge can be considered proportional to the perturbation of electron temperature. [44] Equation (63) shows that the change of ionization rate can also be considered directly proportional to the change of electron temperature for small perturbations. These changes of light emitted and ionization rate with electron temperature are important to mathematical formulation of the striation processes, and to interpretation of experimental results.

Recombination of electrons and ions in the volume of the positive column is negligible compared to the rate at the tube walls. Considering the requirements for conservation of energy, linear momentum, angular momentum and spin, it is evident that the surface atoms of the tube wall provide much better opportunities for these conditions to be satisfied. It is thought that ions and electrons arrive at the walls separately and the recombination takes place through motion along the walls. [37] Since this seems to have no bearing upon the processes of the discharge

involved in these experiments, it will not be considered further.

4. Mobility and Diffusion

When electrons and ions move through a neutral gas as the result of an electric field, their average drift velocities are given by

$$|v|_{\pm} = \mu_{\pm} E$$

The mobility constant for ions / electrons, $\mu_{\pm}$, is a function of the mean free path and average thermal velocity [40]

$$\mu_{+} = 0.75 \frac{e \lambda_{+}}{M_{+} \bar{c}_{+}} \left(\frac{M_{+} + M}{M}\right)^{\frac{1}{2}}$$

$$= 1.06\ e\ \lambda_{+} / M_{+} \overline{c_{+}} \qquad (64)$$

$$\mu_{-} = 0.75\ e\ \lambda_{-} / m\overline{c_{-}} \quad . \qquad (65)$$

These are results of derivations by Langevin, and the ionic mobility is quite satisfactory. Loeb [37] has improved the electron mobility expression, but the formula given above provides values which are satisfactory to an order of magnitude, and has the advantage of being more easily understood. Using values of mean free path and average electron energy given in chapter IV, the following values of mobility can be calculated:

$$\mu_{+} = 1.24 \times 10^{4} \quad (cm^2/volt\ sec)$$

$$\mu_{-} = 80 \times 10^{4} \quad (cm^2/volt\ sec)$$

Note that the electron mobility is much higher than the ion mobility. This is due primarily to the lower electronic mass, as may be seen from a comparison of the two mobility formulas.

Mobility is also important in the diffusion processes of the positive column. Since most recombination of ions and electrons produced

in the column takes place at the walls of the discharge tube, a radial concentration gradient exists in the tube. Electrons and ions tend to diffuse toward the walls with their motion governed by concentration gradients and electric fields according to the equation

$$\vec{\Gamma}_{\pm} = - \nabla (D_{\pm} N_{\pm}) \pm N_{\pm} \mu_{\pm} \vec{E} \ . \tag{66}$$

The opposite signs arise from the difference in signs of the charges. In the steady state, particle flux of each type must be equal, and the plasma condition forces $N_{+} \approx N_{-}$. If the electron temperature across the tube is constant as is essentially the case, $D_{\pm}$ is no longer a function of position. [17] The electric field can then be eliminated from the equation giving

$$\vec{v}_{\pm} = \frac{-(D_{+}\mu_{-} + D_{-}\mu_{+})}{\mu_{+} + \mu_{-}} \cdot \frac{\nabla N}{N} \tag{67}$$

$$= - D_{a} \cdot \frac{\nabla N}{N} \tag{68}$$

Diffusion of this type is called ambipolar diffusion, and if $T_e >> T_i$ (as is the case in this work), the coefficient of ambipolar diffusion can be simplified [17] to

$$D_{a} \approx \frac{D_{-}\mu_{+}}{\mu_{-}} \tag{69}$$

Mobility and diffusion play an important role in forming local space charges in the positive column, which then change the electric field, electron temperature and in turn the ionization rate. Pekarek has investigated this, beginning with continuity equations for ions and electrons and the Poisson equation. [53] By assuming perturbations of the form

$$N_{\pm} = N_{o\pm} + n_{\pm} \qquad |n| << N_o \tag{70}$$

$$E = E_o + e \qquad |e| << E_o \tag{71}$$

these equations can then be written

$$\frac{\partial n_+}{\partial t} = D_+ \frac{\partial^2 n_+}{\partial x^2} - \mu_+ E_o \frac{\partial n_+}{\partial x} - \mu_+ N_o \frac{\partial e}{\partial x} + Q \tag{72}$$

$$\frac{\partial n_-}{\partial t} = D_- \frac{\partial^2 n_-}{\partial x^2} + \mu_- E_o \frac{\partial n_-}{\partial x} + \mu_- N_o \frac{\partial e}{\partial x} + Q \tag{73}$$

$$0 = \frac{\partial e}{\partial x} - 4\pi q_o \cdot (n_+ - n_-). \tag{74}$$

Since ion concentration changes much more slowly then electron concentration, the ion concentration is assumed given. Substituting equation (74) into (73) results in the differential equation

$$\frac{\partial n_-}{\partial t} - D_- \frac{\partial^2 n_-}{\partial x^2} + \mu_- E_o \frac{\partial n_-}{\partial x} + \mu_- N_o \cdot 4\pi q_o n_-$$

$$= Q + 4\pi Q_o N_o n_+ \tag{75}$$

Under the assumption that $Q = 0$ and a Dirac δ-function initial ion perturbation, it is shown that the relaxation time for the electron distribution to be established is given by

$$\tau_- \approx \frac{\lambda_D^2}{D_-} \cdot \tag{76}$$

For the conditions of this experiment

$$\lambda_D^2 = 5.0 \times 10^{-5} \text{ cm}$$

$$D_- = 1.8 \times 10^{6} \text{ cm}^2/\text{sec}$$

$$\tau_- = 2.8 \times 10^{-11} \text{ sec}$$

Characteristic frequencies for moving striations are of the order of 0.5 - 50 kHz. Electron relaxation time is several orders of magnitude

shorter than times associated with changes of striation parameters. The electron density thus follows that of the ions rapidly enough to consider it quasi-static. With this result, the electron density can be written in terms of the ion density as

$$n_-(x, t) = \int_{-\infty}^{\infty} G_-(x - \xi) \cdot n_+(\xi, t)\, d\xi \tag{77}$$

where

$$G_-(x) = \frac{\ell_D'}{2\lambda_D^2} \cdot e^{-x/\ell_1} \cdot e^{-|x|/\lambda_D} \tag{78}$$

and

$$\lambda_D = \text{Debye length} \quad (\text{eq. } 60)$$

$$\ell_1 = 2D_-/\mu_- E_o \tag{79}$$

$$\ell_D' = \left(\frac{1}{\lambda_D^2} + \frac{1}{\ell_1^2}\right)^{\frac{1}{2}} \tag{80}$$

and the space charge is then given by the equation

$$\rho(x, t) = q_o \int \left[\delta(x - \xi) - G_-(x - \xi)\right] \cdot n_+(\xi, t)\, d\xi \,. \tag{81}$$

Equation (81) shows that the space charge is different from zero whenever $n_+ \neq 0$. Its magnitude depends upon n_+ and the plasma parameters through equation (78).

There is another consequence of the ion perturbation. The space charges which are formed create electric fields which perturb the main dc field. Since the electric field determines the electron temperature through the equation

$$\frac{-\partial U_e}{\partial x} = \frac{3}{2} E - \frac{16}{3\pi} \frac{U_e^2}{E\lambda_e^2} K^* \tag{82}$$

where

U_e = electron energy in eV

λ_e = electronic mean free path

K^* = mean energy loss of the electron in an elastic collision ,

the change of electric field also changes the electron temperature. Pekarek analyzed this change as a function of distance by introducing perturbations of electric field and electron temperature through the relations [51]

$$U_e = U_{e_o} + \theta \qquad |\theta| << U_{e_o} \tag{83}$$

$$E = E_o + e \qquad |e| << E_o \tag{71}$$

The spatial change of electron temperature becomes

$$\frac{\partial \theta}{\partial x} = a_1 \theta - b_1 e \tag{84}$$

if second order terms are neglected. In arriving at this relation, the quantity U_{e_o} is equated to the energy gained from the electric field in a mean free path. The constants a_1 and b_1 are

$$a_1 = \frac{16}{3\pi} \frac{U_{e_o}}{E_o \lambda_e^2} \left(2K^* + U_{e_o} \frac{\partial K^*}{\partial U_e}\right) \tag{85}$$

$$b_1 = \left[\frac{3}{2} + \frac{16}{3\pi} \cdot \frac{U_{e_o}}{E_o \lambda_e}\right] q_o \tag{86}$$

The importance of equation (84) is the shift of electron temperature maximum from electric field maximum. Pekarek has shown that this spatial phase difference is essential to amplification of the wave of stratification. [51]

Since a change of electron temperature also changes the light emitted by the discharge, variations in light emitted along the discharge can be attributed to temperature gradients, local changes in electric field, and ultimately to regions of local space charge.

The formation of space charges and electron temperature gradients also changes the diffusion processes. During the derivation of the ambipolar diffusion coefficient, it was assumed that the electron diffusion coefficient was constant as electron temperature is nearly constant across the tube. A temperature gradient along the column means that a perturbation of ion density will decay through electron temperature diffusion as well as through ambipolar diffusion. In order to compare the magnitudes of these terms, Pekarek and Krejci [55] write equation (66) in its full form

$$\Gamma_- = (D_-)\nabla N_- + (N_-)\nabla D_- + E\mu_- N_-$$

and denote the ratio of the terms of interest by

$$R = \frac{N_-(\nabla D_-)}{D_-(\nabla N_-)} \tag{87}$$

noting that the diffusion previously discussed occurs when $R \ll 1$. Expanding the diffusion coefficient about the equilibrium temperature and making use of the relations

$$D_- = kT_-\mu_- / q_o \tag{88}$$

$$\theta = k(T_- - T_{-o}) \tag{89}$$

the expression for R becomes

$$R = \frac{N_{-o}\nabla\theta}{kT_{-o}\nabla n_-}\,\gamma \tag{90}$$

where

$$\gamma = 1 + \frac{kT_{-o}}{\mu_{-o}}\left(\frac{\partial \mu_-}{\partial kT_-}\right)_{T_{-o}} \tag{91}$$

Except for the case of elastic collision cross-section increasing linearly with electron energy, (making $\gamma = 0$), γ is of the order of one, and may be positive or negative. Thus determination of R depends upon

the quotient $\nabla\theta/\nabla n_-$. Equation (77) gives the form of the electron density curve, and a similar equation describes the electron temperature as a function of position

$$\theta = \int_{-\infty}^{\infty} G_\theta\,(x - \xi)\; n_+\,(\xi)\; d\xi \qquad (92)$$

where

$$G_\theta(x) \approx G_\theta^o = 2\pi q_o \cdot b_1 \cdot \left[\frac{\lambda_D}{1 + a_1 \lambda_D}\; e^{-x/\lambda_D} \cdot U(x) \right.$$

$$\left. + \frac{D}{1-a_1\lambda_D}\; e^{x/\lambda_D} \cdot U(-x) - \frac{2a_1 \lambda_D^2}{1-(a_1\lambda_D)^2}\; e^{a_1 x} \cdot U(-x) \right] . \qquad (93)$$

Calculating the gradients of θ, n_- for a sinusoidal ion density perturbation with wavelength much larger than λ_D gives the result

$$R = \frac{b_1}{q_o}\; \gamma . \qquad (94)$$

An earlier paper showed [51]

$$b_1 = 3q_o/2 .$$

The value of R is thus of order one. This means that diffusion of electrons by temperature gradient is of the same order of magnitude as diffusion due to a concentration gradient.

Investigation of these discharge processes has come about as a result of research into moving striations. Some are applied to this work to explain experimental results. Others, such as the diffusion of electrons due to a temperature gradient, have not yet been applied to striation work.

APPENDIX II

WAVES OF STRATIFICATION

This section gives a brief description of waves of stratification and the various theories which have been set forth before reporting work on irradiation of the discharge by an external source. Parameters of acoustically excited waves of stratification are also presented.

A. Theory of the Wave of Stratification

Several attempts to describe mathematically the development of the wave of stratification on the basis of the microphysical processes of the positive column have been set forth. The earliest of these works was published by Pekarek in 1957. [43] In this approach, the observed structure of the wave is postulated, the changes of electric field and space charge are related to this structure, and the production and decay of the space charges are included by relaxation times characteristic of the processes involved. Each maximum and minimum of light intensity is indexed so that the light area numbered 2k is actually the k^{th} light area (figure 1-1). Perturbations of steady state quantities are denoted by

θ electron temperature

n charged particle density

m metastable atom density

q space charge density,

and the constants α, β, are introduced to describe the decay of space charge to zero and the removal of the metastable perturbation by ionization.

With these quantities describing the column, and assuming the light intensity changes to follow those of the electron temperature, the

periodic changes in the plasma are described by two chains, depending on whether the ionization is predominantly stepwise or direct. Both chains begin with a change of electron temperature which is assumed to be accompanied by a change in ionization rate:

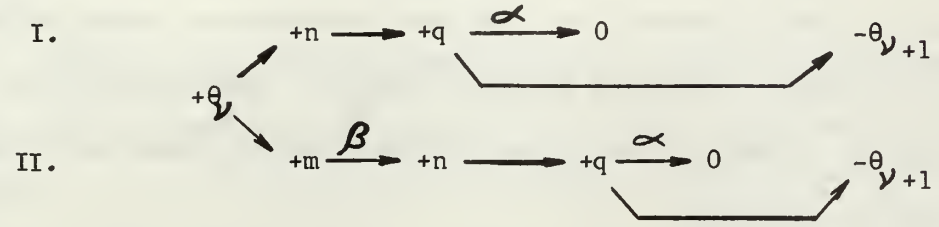

In chain I, direct ionization is assumed to produce an increase in the number of charged particles of both signs, and space charges form due to the higher mobility of the electrons. These space charges decay to zero with relaxation time $\tau_1 = 1/\alpha$, but cause a change in electron temperature of opposite sign in the adjacent region on the anode side. In chain II, metastable atoms produced by the increase in electron temperature are ionized in a characteristic time $\tau_2 = 1/\beta$. From this stage, the processes proceed as in chain I.

It is convenient to use a coordinate system in which the striations are stationary for writing the equations which describe these processes, and transform the solution back to the laboratory frame (in which the striations are moving) after the solution is obtained. Using this method, the following equations can be written:

Chain I

$$\frac{dn_\nu}{dt} = A'\theta_\nu - \alpha n_\nu \tag{95}$$

Chain II

$$\frac{dm_\nu}{dt} = B'\theta_\nu - \beta m_\nu \tag{96}$$

$$\frac{dn_\nu}{dt} = \gamma m_\nu - \alpha n_\nu \tag{97}$$

For both chains, the electron temperature is assumed to follow any change of electric field immediately. The equation expressing this is

$$\theta_{\nu}(t) = -\xi' q_{\nu-1}(t) = -k' \cdot n_{\nu-1}(t). \tag{98}$$

The second equality states that the space charges are formed whenever there is a change in charged particle density. Substituting this equation into the equations describing chains I and II gives the following differential equations:

I
$$\frac{d\theta_{\nu}}{dt} + \alpha\theta_{\nu} = -\alpha A\theta_{\nu-1} \tag{99}$$

II
$$\frac{d^2\theta_{\nu}}{dt^2} + (\alpha + \beta)\frac{d\theta_{\nu}}{dt} + \alpha\beta\theta_{\nu} = -B_o\theta_{\nu-1}. \tag{100}$$

These equations are solved under the initial condition of a Dirac delta function increase of the electron temperature, and the solution gives the time development of electron temperature in each of the numbered regions. The time of occurrence of the maximum amplitude of each region is determined, as are the times of occurrence of half maximum intensity. Since the time of occurrence of the maximum of light intensity is related to the propagation velocity of the wave (u) and the striation velocity (v), both of which are measurable quantities, and are related in turn to the relaxation times through the striation spacing or wavelength (λ), the relaxation times can be checked from the experimentally determined values for agreement with the hypotheses as to the governing processes in each chain. This determination of relaxation time has been a most useful result. It can be shown that

$$\tau_o = \frac{\lambda}{2} \cdot \frac{1}{u + v} \tag{101}$$

where the relaxation time is related to the plasma processes through

$$\tau_o = \frac{1}{\alpha} + \frac{1}{\beta} = \tau_1 + \tau_2 \qquad (102)$$

for cases in which there are two processes. Also predicted by this theory are

(a) oddness of the wave of stratification (initial conditions of opposite sign produce waves of stratification with light and dark areas reversed)

(b) a spatial decrease in amplitude of the wave group followed by an increase when the amplification is larger than 1.0

(c) direct dependence of wave of stratification amplitude upon the amplitude of the initial disturbance

(d) growth of width of the packet in time according to $t^{\frac{1}{2}}$.

These predictions were verified in a later experimental work, with the exception of the width of the packet of the fast wave. [48] The experimental results in this case agreed with theoretical predictions in form although not in magnitude.

It should be emphasized that this theory takes the layered structure as a basis, attributes the light intensity variations to changes in electron temperature, and attributes ensuing changes in electron temperature to the space charges produced by the higher mobility of the electrons. Basic microphysical processes in the positive column are not used to predict the response of the plasma to the perturbation of ionization rate.

A later theoretical work uses a simplified form of Poisson's equation and the equation of continuity for ions with only production of ions due to changes in the ionization rate being considered. [51] The Debye

length is essentially assumed infinite, as the electrons arising from the perturbation of the ionization rate are assumed to diffuse immediately upon being created. Perturbation relations of the form

$$E = E_o + e \qquad |e| \ll E \tag{71}$$

$$N = N_o + n \qquad |n| \ll N \tag{70}$$

substituted into these equations give the equations

$$\frac{\partial e}{\partial x} = 4\pi q_o n_+ \qquad \text{(esu)} \tag{103}$$

$$\frac{\partial n_+}{\partial t} = \bar{z}' N_o e \tag{104}$$

where $\bar{z}'$ is the rate of change of ionization rate with electric field, and q_o is the electronic charge. The solution to this system of equations under the initial condition of a unit step in ion density in both time and space is a Bessel function with the product $(xt)^{\frac{1}{2}}$ as the argument. With coordinate axes chosen such that positive X is in the direction of the electric field, and axes designated as in the time-space diagram of figure 1-1 (negative X in the vertical direction), periodic solutions arise in the form of a family of hyperbolae (figure 4-2). If very short and very long wavelength striations are excluded from consideration by drawing the dotted lines shown approximately 15 degrees either side of the quadrant bisector, the resulting lines have the general appearance of the wave of stratification. This diagram then shows the propagation in the cathode to anode direction, the motion of striations in the cathode direction, and convex dispersion of the wave (discussed later).

This simple set of equations thus contains the necessary processes

for the propagation of a periodic structure with the properties of the wave of stratification, provided short and long wavelengths are eliminated. An improved treatment must include these processes. Pekarek lists the three important physical processes which cause the wave of stratification as

(a) dependence of the ionization coefficient on the electric field in the plasma

(b) the production of space charges due to different diffusion rates of the charged particles

(c) creation of additional electric fields due to the creation of space charges.

Since perturbation of the electric field causes a perturbation of the electron temperature, the ionization rate is dependent upon electron energy. Later formulations have used this dependence instead of the dependence upon electric field. Moreover, the shift of electron temperature maximum from the electric field maximum has been shown to be essential to the amplification of the wave of stratification.[52] If the wave is rapidly attenuated, its characteristics cannot be measured, while large amplification causes nonlinear behavior of the wave, invalidating the assumptions of the linearized theory. Thus the behavior of the electron temperature is important.

Pekarek and Krejci base an extensive theoretical work on the equations of continuity of ions and electrons, the equation for electron temperature variation in a spatially varying electric field, and Poisson's equation. [54, 56] These are written as

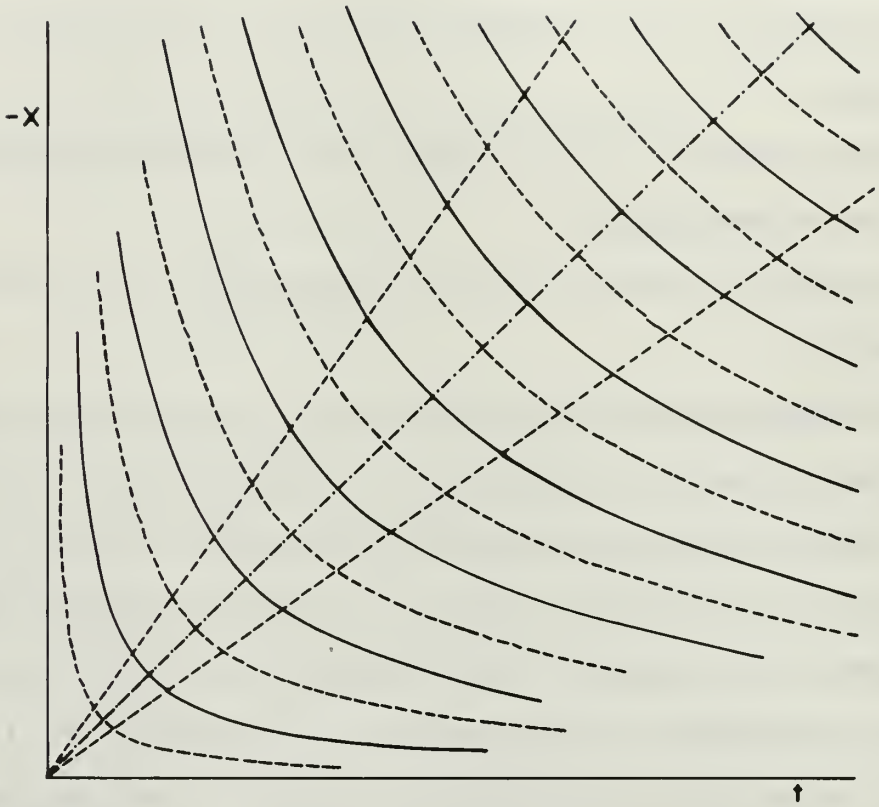

Figure 4-2. Solution to simplified system of equations describing electric field variations in the positive column following unit step initial conditions.

$$\frac{\partial n_+}{\partial t} = D_+ \frac{\partial^2 n_+}{\partial z^2} - \mu_+ N_o \frac{\partial e}{\partial z} - \mu_+ E_o \frac{\partial n_+}{\partial z}$$

$$- \frac{1}{\tau_a} (n_+ - n_-) + z'_\theta N_o \theta \qquad (105)$$

$$\frac{\partial n_-}{\partial t} = D_- \frac{\partial^2 n_-}{\partial z^2} + \mu_- N_o \frac{\partial e}{\partial z} + \mu_- E_o \frac{\partial n_-}{\partial z}$$

$$+ z'_\theta N_o \theta \qquad (106)$$

$$0 = \frac{\partial e}{\partial z} - 4\pi q_o (n_+ - n_-) \qquad (74)$$

$$0 = \frac{\partial \theta}{\partial z} - a_1 \theta + b_1 e \qquad (84)$$

Perturbations of the form given in equations (70), (71), and (83) have been applied. The terms $z'_\theta N_o \theta$ and $\frac{1}{\tau_a}(n_+ - n_-)$ represent production of particles due to a change in ionization rate and loss due to ambipolar diffusion. The term $z'_\theta N_o \theta$ was present in the simple set of equation (eqs. (102), (103)) which produced the time-space periodic structure of figure 4-2. This set included no damping mechanism. Ruzicka and Pekarek carried out a solution to the set of equations given above with the term $z'_\theta N_o \theta$ deleted. [70] The system in this case gave only a monotonic decay of an aperiodic disturbance in ion density, indicating that the change of ionization rate with electron temperature is a necessary condition for the excitation of a wave of stratification.

The equations are simplified for solution in the following manner:

(1) $D_+ \frac{\partial^2 n_+}{\partial z^2}$ is neglected as the changes of ion density due to additional electric fields will be larger than the diffusion due to concentration gradient

(2) $\frac{\partial n_-}{\partial t}$ and $z'_\theta N_o \theta$ are neglected in the electron balance equation as the change of electron density has been shown to adjust to the change of ion density several orders of magnitude faster than the average lifetime of the charged particles. [53] Electron density is thus quasi-stationary.

(3) the system is transformed to a coordinate system at rest with respect to the ions by $Z = x + \mu_+ E_o t$

(4) the term μ_+ is neglected in the sum $\mu_+ + \mu_-$.

The equations which result are:

$$\frac{\partial n_+}{\partial t} = -\mu_+ N_o \frac{\partial e}{\partial x} - \frac{1}{\tau_a}(n_+ - n_-) + Z'_\theta N_o \theta \tag{107}$$

$$0 = D_- \frac{\partial^2 n_-}{\partial x^2} + \mu_- E_o \frac{\partial n_-}{\partial x} + \mu_- N_o \frac{\partial e}{\partial x} \tag{108}$$

$$0 = \frac{\partial e}{\partial x} - 4\pi q_o (n_+ - n_-) \tag{74}$$

$$0 = \frac{\partial \theta}{\partial x} - a_1 \theta + b_1 e \ . \tag{84}$$

These equations receive no further simplification before a general solution is obtained. The processes included in these equations are

(a) change of ionization rate with electron temperature

(b) creation of space charges due to different free diffusion rates of ions and electrons

(c) creation of additional electric fields due to creation of space charges.

These were shown to be sufficient for the formation of a periodic time-space structure. Also included are terms for

(d) the displacement of electron temperature with respect to electric field (necessary for amplification of the wave of stratification)

(e) damping of the striations by ambipolar diffusion

(f) finite diffusion coefficient of electrons

(g) finite mobility of electrons

(h) ionic mobility

(i) effect of electron density on ionization rate.

The time and space development of the ion density in terms of these basic processes is obtained by using the 2-sided Laplace transform described in [61]. The equation which results is:

$$\frac{\partial n_+}{\partial t}(x, t) = \int_{-\infty}^{\infty} K(x - \xi) \cdot n_+(\xi, t) \cdot d\xi - \frac{1}{\tau_\mu} n_+ . \qquad (109)$$

In this equation, the term $K(x - \xi)$ is a sum of three exponential functions. The equation in this form is very difficult to solve. By assuming that the Debye length is nearly zero, the authors are able to make simplifications and finally arrive at the following equation:

$$\frac{\partial n_+}{\partial t}(Z, t) = \frac{kT_-}{q_o} \mu_+ \frac{\partial^2 n_+}{\partial Z^2} + z'_\theta b_1 \frac{D_-}{\mu_-} \cdot n_+$$

$$- A_{10} \int_{-\infty}^{\infty} e^{a_1(Z - \xi)} U(-Z + \xi) \, n_+ (\xi, t) \, d\xi . \qquad (110)$$

Their analysis of each term on the right hand side of the equation is important and can be summarized as follows:

(a) the first term is a diffusion term which damps the very short wavelength striations

(b) the second term makes amplification possible (note that $b_1 = 0$ means full damping)

(c) the integral gives an oscillatory character to the solution and also damps the long wavelength striations (through the term

a_1), therefore

(d) there are no redundant terms in this equation. All the major physical characteristics are present, and any additional terms can only modify the solution, but not alter its basic form.

Solution of this equation under a Dirac δ-function disturbance of ion density at time t = 0 has the form

$$n_+(Z, t) = \frac{n_o}{2\pi} \int_{-\infty}^{\infty} \exp\left[i(kZ - \omega(k)t) + \phi(k)t\right] dk \qquad (111)$$

where

$$k = 2\pi/\lambda$$

λ is striation wavelength

$$\omega(k) = \frac{A_{10}k}{k_1^2 + a_1^2} \qquad (112)$$

$$A_{10} = z'_\theta b_1 (E_o + a_1 \frac{D_-}{\mu_-}) \qquad (113)$$

$$\phi(k) = -k^2 D_a + z'_\theta b_1 \frac{D_-}{\mu_-} - \frac{A_{10} a_1}{k^2 + a_1^2} \quad . \qquad (114)$$

Equation (111) is a Fourier integral over all wave numbers. The term $\phi(k)$ is present as an amplification (or damping) term, and thus shows how the microphysical processes affect striation wavelength. Amplification will be maximum for

$$\left.\frac{\partial \phi(k)}{\partial k}\right|_{k=k_1} = \phi'_1 = 0 \ ,$$

and this gives

$$k_1 = \pm a_1 (\frac{1}{\eta} - 1)^{\frac{1}{2}} \qquad (115)$$

where

$$\eta = + (\frac{a_1^3 D_a}{A_{10}})^{\frac{1}{2}} \qquad (116)$$

Real values of k_1 exist for $0<\eta<1$, and when used in equation (112) give

$$\omega_1 = \frac{A_{10}k_1}{k_1^2 + a_1^2} = \frac{D_a a_1^2}{\eta}\left(\frac{1}{\eta} - 1\right)^{\frac{1}{2}} \tag{117}$$

Wojaczek has discussed a method of solving an integral of the type shown in equation (111). [88] Functions $\omega(k)$ and $\phi(k)$ are expanded in a Maclaurin series about the resonant wave number (k_1) retaining only first order terms. This is valid only for large distances from the point of origin of the wave (large Z), and assumes that there is large damping for all other wavelengths. Using this technique, the integral in equation (111) can be evaluated, giving

$$n_+(Z, t) = \frac{n_o}{(4\pi|B|\,t)^{\frac{1}{2}}} \exp\left[-\frac{(Z - \omega_1' t)^2}{4b_1 t} + \phi_1 t\right]$$

$$\cdot \cos\left[k_1 Z - \omega_1 t + \frac{(Z - \omega_1 t)^2}{4q_1 t} - \frac{\psi}{2}\right] \tag{118}$$

where

$$b_1 = \frac{\omega_1''^2 + \phi_1''^2}{-2\phi_1} \qquad q_1 = \frac{\omega_1''^2 + \phi_1''^2}{2\omega_1'}$$

$$B = \frac{1}{2}(\omega_1''^2 + \phi_1''^2)^{\frac{1}{2}} \qquad = \tan^{-1}\left(\frac{-\omega_1''}{\phi_1''}\right)$$

The authors plot the solution as a function of time for a given coordinate, noting that the plot has the typical form of the wave of stratification (figure 2-3(a)). Group and phase velocities obtained from the customary relations

$$v = \frac{\omega_1}{k_1} = D_a \frac{a_1}{\eta} \tag{119}$$

$$u = \frac{\partial \omega}{\partial k} = -D_a \frac{a_1}{\eta}(1 - \eta) \tag{120}$$

are of opposite sign. The wave has anode-directed group velocity, (due to the negative sign) and is thus of the general nature of the wave of stratification. By using striation wavelength and frequency obtained experimentally, together with an estimated relaxation length ($1/a_1$) for electron temperature, the quantities calculated from equations (118, 119) and (120) are found to agree with the observed values of these to within an order of magnitude. This theory therefore provides a satisfactory description of the wave of stratification for pressures of a few torr and currents of order of an ampere.

Since the phase and group velocities are of the same order of magnitude, and $|u| \leq |v|$, this theory is inapplicable to the slow and fast waves observed at lower currents. It also predicts a monotonic decay of light intensity on the cathode side of the initial disturbance.

Lee, Bletzinger and Garscadden have solved equation (110) by using a Fourier series technique. [36] Their results show one significant difference, in that a forward wave, propagating from anode to cathode, is predicted whenever $\lambda < 2\pi/a_1$. This has recently been observed in experiments on a 35 torr argon discharge. [20]

Wojaczek has made theoretical and experimental investigations of small amplitude moving striations and waves of stratification. [84-86, 88-90]. Using conservation equations for electrons and ions, Poisson's equation and the equation for energy balance of the electrons (including thermal conductivity), he assumes small perturbations of the variables with plane wave time and space dependence. A dispersion relation is obtained, and with the assumption of a complex wave number, amplification as a function of frequency is derived. [88] Comparison with experiment shows good agreement in form for both the amplification and dispersion.

A plot of $R \cdot \omega_o$ against $R \cdot p_o$, where

R = tube radius

ω_o = resonant frequency

p_o = pressure

gives a curve which is in good agreement with experiment for small values of $R \cdot p_o$. Pupp's earlier experiments also gave data which fit this curve. [66]

Dispersion is the variation of phase velocity with wavelength (or frequency). A dispersion curve is usually constructed with the frequency (ω) as a function of the wave number ($k = 2\pi/\lambda$). Figure 4-3 shows such a curve. Since the phase velocity and group velocity can be calculated from the relations

$$v = \omega/k \tag{119}$$

$$u = \partial\omega/\partial k, \tag{120}$$

the dispersion curve is useful in determining the propagation characteristics of the wave of stratification. Krejci and Pekarek have analyzed the combinations of backward and forward waves and their associated dispersion curves. [34] In their work it is shown that the curvature of the striation paths also determines the curvature of the dispersion curve at the point of the resonant wavelength. Figure 44 shows the idealized forms of the waves of stratification in (a) neon, and (b) a neon-hydrogen ($\sim 7/1$) mixture. The ratio of group and phase velocities in each wave are approximately the same; magnitudes are different. Dispersion is different in that the lines are curved away from the origin (convex) in (a), and toward the origin (concave) in (b). The portion of the dispersion curve corresponding to each of these cases is shown in figure 4-4. This dispersion curve is predicted by the solution to equation (111). In

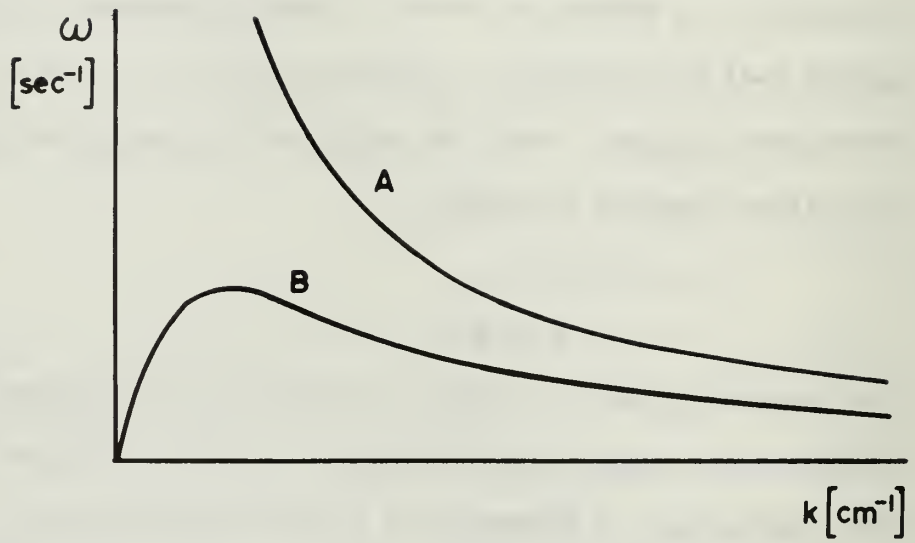

Figure 4-3. Dispersion curves given by

(a) simplified model with infinite Debye length

(b) finite Debye length theories.

Diagram after Pekarek. [60]

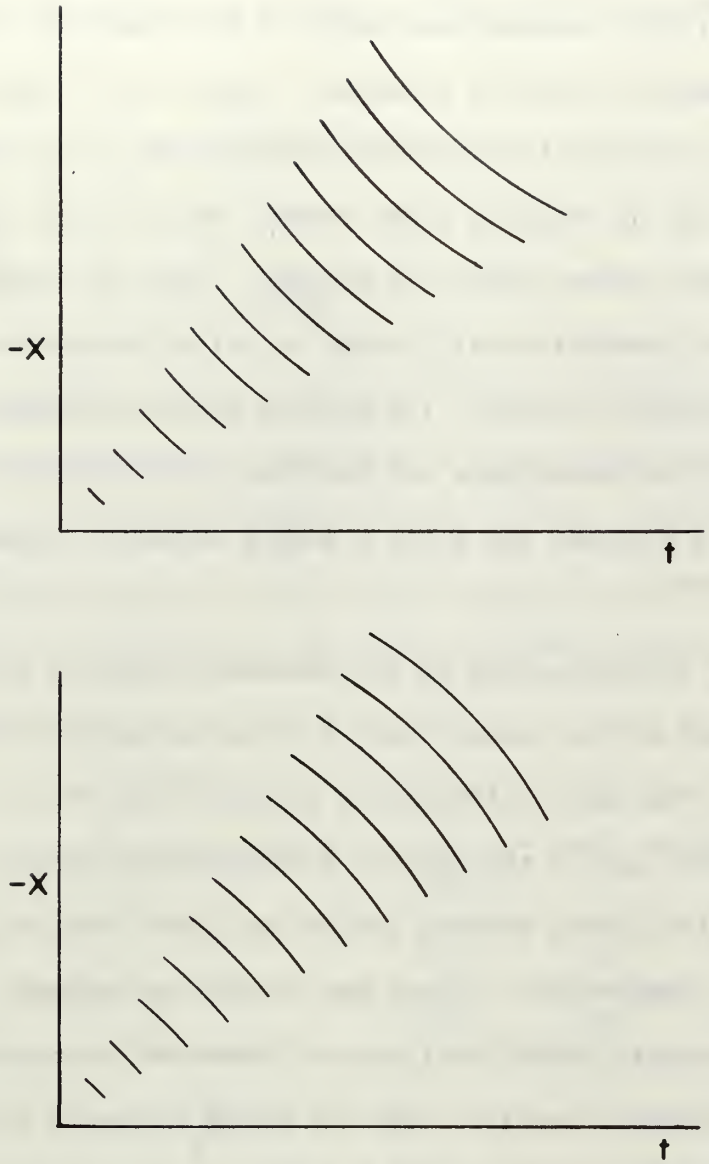

Figure 4-4. Time-space development of light intensity in discharges in (a) neon, (b) neon-hydrogen, following an impulsive perturbation of ion density at the point X = 0, t = 0.

most cases, however, the resonant wavelength is such that the convex portion of the dispersion curve is observed. Curve (a) of figure 4-3 is predicted by the solution to equations (103) and (104). The assumption in the latter case was an infinite Debye length, while in the curve designated (b), a zero Debye length was assumed. Thus the plasma processes have not been formulated well enough to allow information to be derived from the dispersion curve. The authors outline a method for obtaining data from the photographs and constructing dispersion curves, and this both sets a standard and gives a simple method of accomplishing this work.

Pekarek offers an explanation of the concave dispersion in the neon-hydrogen mixture, and of the anode-directed striation motion in pure hydrogen. [59, 60] The basic differential equation (eq. 110) has a quadratic ionization term, and in the case of a finite Debye length, this term may shift the ionization maximum toward the anode from the point of maximum electron temperature. Since the ionization maximum is shifted toward the anode, electric field will also be increased in this direction, causing the temperature to increase, and the chain of events to recur. This is the tentative explanation which he offers for anode-directed striation motion in hydrogen. For the case of the mixture, contribution from the quadratic ionization term increases as striation amplitude increases, giving a larger anode-directed component to the striation velocity at the larger amplitude phase of the striation. Thus, the case of concave dispersion is thought to be associated with non-zero Debye length.

B. Striation Boundaries

An empirical relation for the upper and lower striation boundaries

is given by Rutscher and Wojaczek. [69] Using the formulas given for the upper

$$i_l = \frac{A_l}{p^{\lambda}} + B_l$$

and lower

$$i_s = \frac{A_s}{p - B_s}$$

boundary currents, it is possible to make calculations for the tubes used in this experiment. (Subscripts l and s come from the German words "langsam" and "schnelle", meaning slow and fast, respectively. Slow and fast striations usually arise at the respective boundaries.) Quantities are defined as follows for neon, with p given in torr and tube radius in centimeters:

Radius	A_l	B_l	λ
1	8.0	.1	2.43
2	6.6	.07	1.83
3	6.4	.06	1.59

$$A_s = \frac{a_s}{R^{\alpha}} \qquad a_s = .24$$

$$\alpha = .63$$

$$B_s = \frac{b_s}{R^{\beta}} \qquad b_s = .93$$

$$\beta = 1.1$$

For tube I, R = 1.0, and for tube II, R = 2.5. Tube I was used in the irradiation experiments, tube II in the acoustic experiments. If we assume the following values for tube II, which can be obtained from this table by interpolation, then the striation boundaries can be calculated

$$A_l = 6.5 \qquad \lambda = 1.71$$

$$B_l = 0.65$$

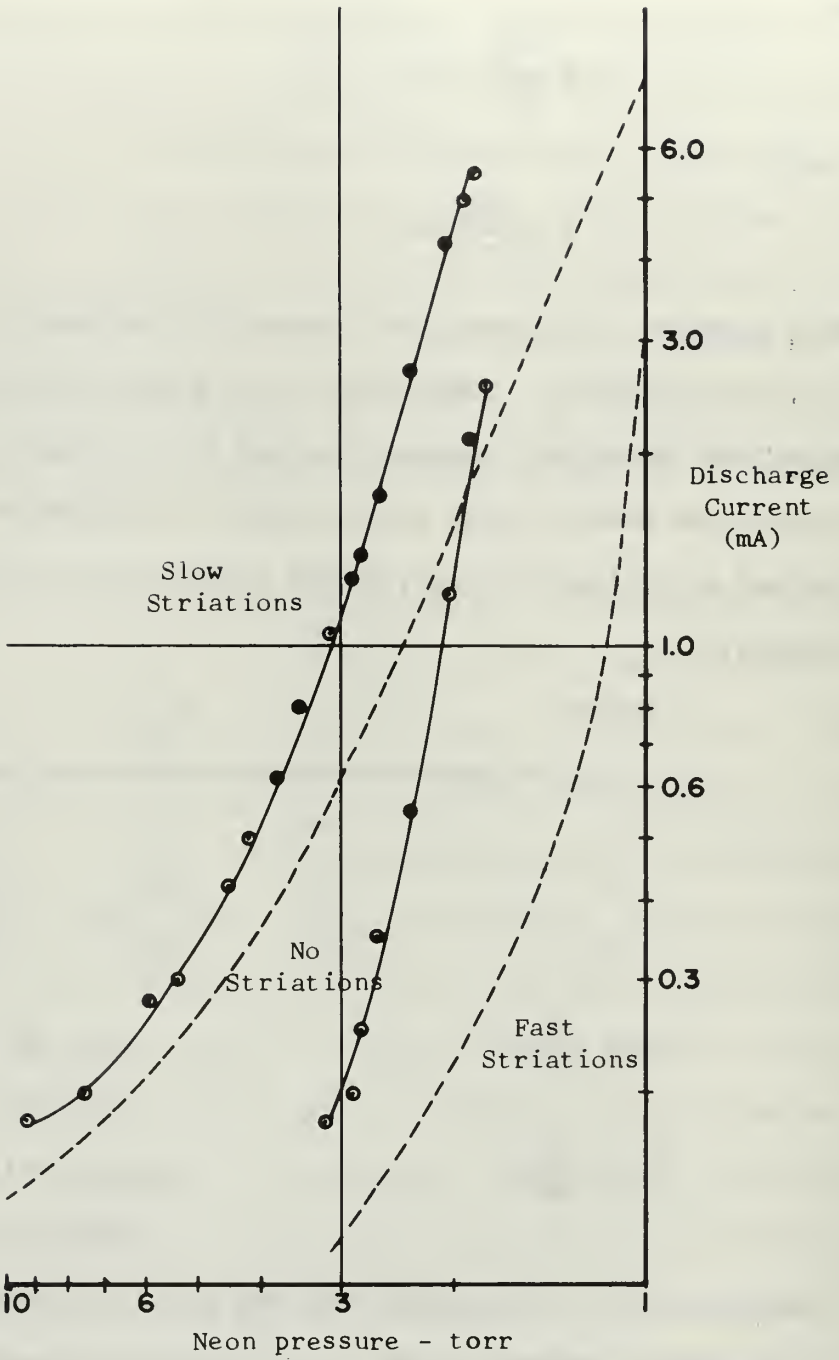

Figure 4-5. Boundary currents for striation-free operation as a function of pressure in tube I. Diameter: 1 cm, length 30 cm.

for each of the tubes. Results are plotted in figures 2-3 and 4-5 as dotted lines, and the experimentally determined values are shown as points with a curve drawn through to allow comparison with the results of this calculation. It is evident that the striation boundaries found in this experiment are much different from those predicted by the empirical relationships. In all cases the experimental boundaries occur at larger currents, and are as much as an order of magnitude larger in the case of the lower boundary. With the exception of the one cm tube at the upper boundary, all experimental points fall in such a manner that a straight line is the most obvious approximation to the current-pressure dependence on the logarithmic plot.

C. Waves of Stratification Excited by Acoustic Waves

Table A-1 shows the general increase in both velocity of propagation of the waves (u_p, u_r) and speed of the individual striations (v_p, v_r) as pressure is decreased. Subscripts p and r are commonly used to designate the slow and fast waves. The fast wave recorded at 0.82 torr may have been an s wave. Wave propagation velocities are accurate only to 15% to 20% because amplification is large in many cases, and at times two waves have probably merged. These factors make it difficult to determine the maximum of the wave group amplitude, and the packets are wide enough that the method given by Krejci and Pekarek in [34] cannot be successfully applied. In cases where the sound wave was propagated in the cathode to anode direction, this acted to increase the apparent group velocity, and the acoustic wave also gave rise to the striations. Striation velocity measurements are accurate to 5 to 10%, and wavelength accuracy is about 10%.

Four general variations in parameters of the wave group can be obtained

Table A-1

Characteristics of Acoustically Excited
Waves of Stratification

Pressure (torr)	i (mA)	u_p (m/s)	v_p (m/s)	λ_p (cm)	u_r (m/s)	v_r (m/s)	λ_r (cm)
4.0	0.3	36	8.2	2.4	160	35	4.4
4.0	0.2	x	4.8	2.0	140	28	4.2
3.3	0.6	64	6.9	2.3	x	33	4.5
2.7	0.75	50	7.0	2.4	220	39	4.3
2.7	0.50	65	4.9	2.1	235	28	3.9
2.5	0.60	49	5.5	2.1	x	32	4.1
2.2	3.1	67	20/17	2.8/2.7	x	x	x
2.2	1.6	57	10.5	2.6	x	31	5.1
2.2	1.3	50	9.3	2.5	x	x	x
2.2	0.7	61	5.6	2.3	x	x	x
1.9	1.7	61	11	2.6	x	x	x
1.6	1.7	82	8.4	2.6	x	x	x
1.4	8.0	133	28	2.9	x	x	x
1.4	5.0	108	22	2.9	x	x	x
1.4	2.6	100	13	2.7	x	x	x
1.4	1.5	105	8.5	2.5	x	x	x
1.3	2.6	84	11	2.6	x	x	x
1.0	9.6	140	15	3.0	x	x	x
0.93	4.8	x	14	2.6	x	x	x
0.82	33	220	70	3.0	5000	250	5.4
0.82	10.9	160	36/24	3.0/2.6	x	x	x

Table A-1
(continued)

0.82	10.9	140	24/36	2.7/3.0	x	x	x
0.77	15	140	24	2.9	x	x	x
0.77	10	220	30/21	3.1/2.8	x	x	x
0.77	8.0	220	29/31	3.0/2.7	x	x	x
0.77	5.0	220	21	3.1	x	x	x

from Table A-1: (1) wave propagation velocity (u) decreases with increasing pressure, (2) striation velocity (v) increases with increasing current, (3) striation wavelength decreases with increasing pressure, (4) striation wavelength increases with increasing current. There is no theory which gives satisfactory values of u and v as functions of current and pressure for conditions other than the zero Debye length limit. Early theoretical works of Pekarek related these velocities to plasma parameters through the relaxation time :

$$\tau \doteq \frac{\lambda}{2} \cdot \frac{1}{u + v}$$

In order to compare these predictions of relaxation time with experimental observations, a knowledge of plasma parameters over the experimental range is necessary. The measurements of plasma parameters which were carried out do not cover a sufficient range of current and pressure to allow this comparison to be made.

D. Irradiation of the Discharge

1. Experimental Arrangement

Tube I was filled with 2.6 torr neon, sealed, and mounted parallel to a longer 2.5 cm diameter tube, with a centerline separation distance of 2.1 cm. A strip of black paper approximately 0.6 cm wide was attached to the photomultiplier housing. This encircled tube I to prevent light of the illuminating discharge from entering the slit. A point 10 cm from the anode was chosen for observing the effects of the irradiation upon the light intensity at different values of discharge current. Time-space photographs were taken with 27 cm of photomultiplier travel. Current in the illuminating discharge was 500 mA. A black cloth at times covered the cathode region of the discharge in order to

insure that all effects observed were the result of changes in the positive column, and in each case the cloth had very little noticeable effect on the changes brought about by irradiation.

Peak value of the light emitted by the striations in the illuminating discharge was found to increase as pressure decreased. Light associated with transitions ending on metastable states is the important quantity in this experiment, not total light emitted. Eure has found that intensity of the 8115 Å line in argon increases with increasing pressure. [18] The transition involved in the emission of this line corresponds to that involved in the strong 6402 Å line of neon, with the principal quantum number being four in argon, three in neon. Hence a similar pressure dependence would be expected, and it was found that illuminating discharges had a larger effect upon the discharge in tube I as the pressure was increased. However, Druyvestyn and Penning quote data which show that the fraction of power input to the discharge which is radiated in metastable-ended transitions increases as pressure is increased from 0.1 to 1.0 torr, and decreases as pressure is further increased. [16] Kagan, Lyagushchenko and Khakhaev, working in the pressure range 1-30 torr, also found a monotonic decrease in the total number of transitions which end on metastable states. [31]

The increase of total electrical signal from the multiplier seen in figure 4-6 may be attributed to the change of discharge color from red to orange as the pressure is reduced. Since the S-4 cathode of the 1P21 has a quantum efficiency which is rising rapidly in the color interval red to yellow, the same total number of transitions will cause the electrical signal to be larger when the discharge is more orange (lower pressure).

2. Irradiation Effects on Steady-State Conditions

Figure 4-6 shows variation of light intensity and potential across the discharge tube as a function of discharge current. (A line drawing is given in figure 4-7 to assist in explaining this figure.) In part (a) of figure 4-6, the discharge is not illuminated. Low frequency (slow) striations appear as current is increased above two milliamperes, and high frequency (fast) striations appear below 0.5 milliamperes. Potential across the discharge tube increases as current decreases until the fast striations appear at 0.5 mA. At this point the potential increases less rapidly, indicating that less power is dissipated in the discharge when the fast striations are present. This is in accord with Pekarek's finding that the striated state of the column is a more conservative state. [42] A slight oscillation of the potential across the discharge tube in the presence of slow striations is also evident.

In part (b) of figure 4-6, the discharge is illuminated by a 500 mA, 11.4 torr discharge. The light intensity trace shows that both striation boundary currents have been increased; the lower current boundary from 0.5 to 0.85 mA, and the upper current boundary from 2.05 to 2.15 mA. Striations appearing at the lower boundary have larger amplitudes than in the unilluminated case, while striations appearing at the upper boundary have smaller amplitudes. The striations above the upper boundary appear to have maximum amplitudes which are less well defined than those in part (a) of this photograph. Moving striations were present in the illuminating discharge, and these were unstable due to anode spot oscillations. These oscillations of the illuminating discharge may have caused variation of the amplitude of the slow striations.

a

b

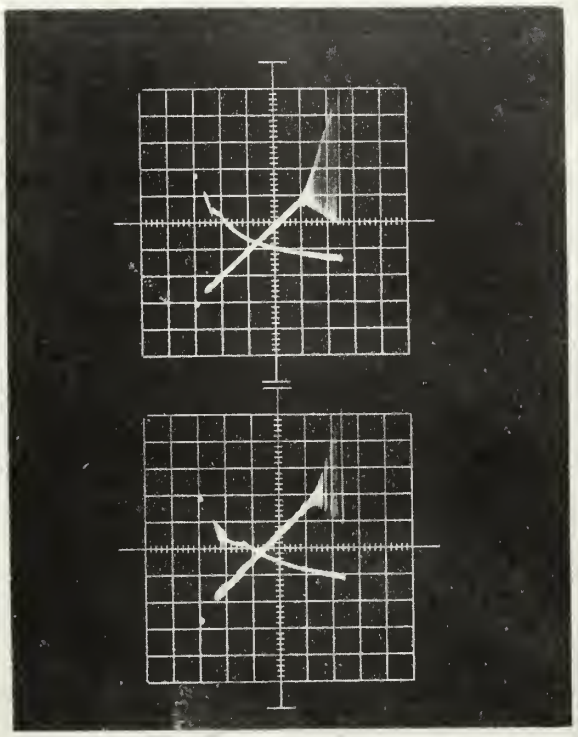

Figure 4-6. Light intensity (increasing to right) and voltage drop across tube I at 2.6 torr. Horizontal scale: 0.5 mA/div. Vertical scale: 20v/div., with the zero of potential offset. Upper - no irradiation. Lower - 500 mA in irradiation discharge.

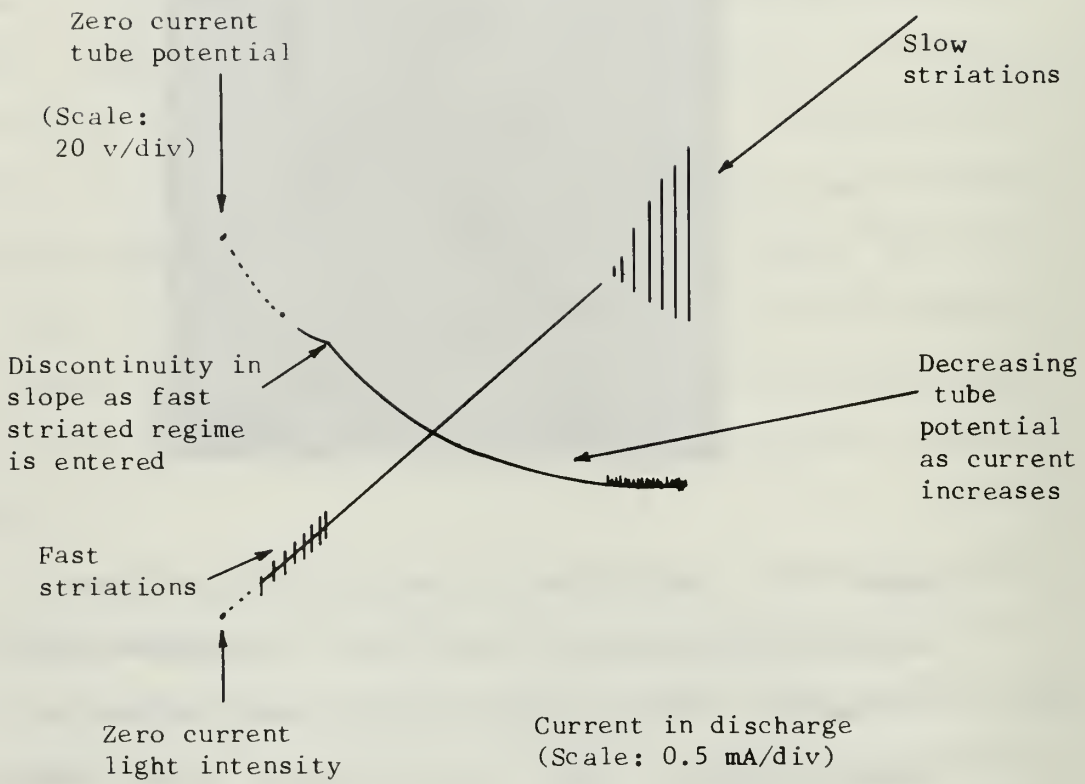

Figure 4-7. Light intensity and potential across the discharge tube as a function of current. This diagram is a key to figure 4-14.

Illumination of the discharge by light from a discharge in the same gas reduces the population of metastable states by promoting atoms in the metastable states to higher energy states from which it is possible to make transitions back to the original state or to another state. Since the population of the metastable states is reduced, the stepwise ionization rate is reduced, requiring an increase in the rate of direct ionization. This must be accomplished through an increase in electron temperature, which in turn is a function of the electric field. The trace of tube potential in figure 4-6 (b) clearly shows this increase of electric potential in the striation-free and slow striation regions. An increase is also present in the current range of the fast striations above a current of 0.5 mA. In this range of current the electric potential across the discharge tube not only increases less rapidly with decreasing current, but is found to decrease immediately below the striation boundary before again increasing as current is further decreased.

Working with this concept of the effect of the illuminating discharge, the decrease of amplitude of the slow striations and increase of the upper current boundary indicate that the slow striations may be associated with metastable atoms. Reduced amplitude of these striations is explained on the basis of the lower population of the metastable levels. Similarly, the increase of fast striation amplitude accompanying the increase of direct ionization under illumination indicates that these striations are associated with direct ionization. Pekarek has also stated both of these possibilities from his relaxation time measurements and from his irradiation experiments. [47, 48]

Total electrical signal from the photomultiplier is higher when the discharge is illuminated. A change of color from red to orange is also

observed, and the higher quantum efficiency of the photomultiplier at shorter wavelengths (discussed earlier) may account for this increase.

3. Irradiation Effects on Waves of Stratification

Figure 4-8(a) shows a slow wave of stratification in tube I for a discharge current of 2.0 mA. Examination of the striation paths from the right hand side of the page (parallel to the paths) reveals convex dispersion in the cathode half of the column, and concave dispersion in the anode half of the column. Part (b) of the figure shows the slow wave propagating in a discharge with the same current. In this case dispersion remains convex throughout the column. Amplification of the wave is also decreased by illumination.

Discussion of dispersion showed that convex dispersion is predicted by zero Debye-length theories, and concave dispersion is presently thought to be due to a quadratic ionization term which shifts the ionization maximum in the direction of the anode. It is therefore attributed to a non-zero Debye length. Since the Debye length exhibits the dependence $\lambda_D^2 \propto T_e/N_o$, an increase in T_e and a decrease in N_e both act to increase λ_D. The change of dispersion observed in the photograph of figure 4-8 would indicate a decrease in Debye length if this explanation were correct.

Assuming that the irradiation effects can be accounted for on the basis of changes in electron density and temperature alone, the following line of reasoning applies:

a) E is increased

b) T_e is increased

c) Since $j = \sigma E$, where

j = current density

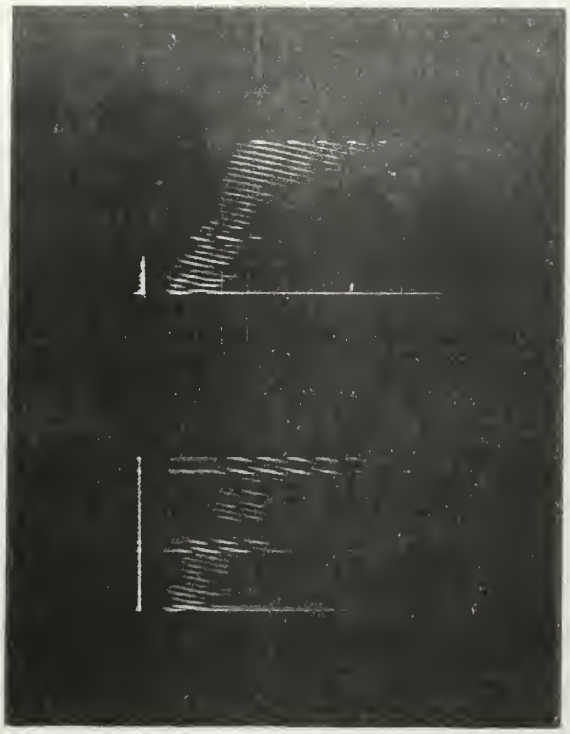

Figure 4-8. Waves of stratification in tube I at 2.6 torr and 2.0 ma. Time: 0.4 msec/div., deflection: 27 cm. Upper - no irradiation, lower - 500 mA in illumination discharge.

σ = plasma conductivity

and $\sigma \propto N_o$.

A constant j requires a decrease in N_o, therefore

d) T_e/N_o is increased, and λ_D is increased.

This, however, is contrary to the expected result.

Before drawing conclusions as to the validity of theoretical ideas relating to dispersion, it must be pointed out that insufficient data is available. The irradiation effects must be examined for several currents in the striation-free region to insure that the phenomenon recorded is a general occurrence. Data collected during this work indicate that concave dispersion is observed less often than convex dispersion. The problem requires further study before a statement can be made.

APPENDIX III

OTHER WORKS ON PLASMA-ACOUSTIC WAVE INTERACTIONS

Suits evidently published the first paper related to this subject in 1935. [81] Using an arc discharge as his main discharge, he excited sound waves by a high-voltage pulsed spark discharge at one end of the arc column, and detected the acoustic waves by observing the variation in electric current drawn in a second spark discharge placed near the other end of the column. From the time required for propagation, he deduced the propagation velocity and hence the neutral gas temperature in the arc. Blum, Dyer and Ingard used this effect of gas pressure on current in their construction of a corona discharge for use as an acoustic transducer. [6] The corona is a special case of a glow discharge, and current drawn for a constant voltage is a function of mobility, which in turn is a function of density. They indicated that this was a sensitive microphone, but as nothing has appeared in the literature other than their abstracts of papers for meetings of the Physical and Acoustical Societies, no quantitative information is available.

Wojaczek inaugurated the present-day form of this work by reporting modulation of the light intensity of the positive column as a result of a high-voltage, microsecond pulse. [87] This was discovered during investigations of the positive column with regard to waves of stratification. He found that the effect was larger when propagation was in the anode to cathode direction. An estimate of the damping showed it to be an order of magnitude larger than that predicted by acoustic wave theory. Hayess performed this experiment for the express purpose of examining the damping coefficient as a function of current and pressure. [25]

Working in xenon, he found that varying the current had little effect on the damping coefficient, and an increase in pressure resulted in a decrease in the damping coefficient. Wall damping was calculated to be the most important influence in the narrow (1.55 cm diameter) tubes used in the experiment. This was an order of magnitude larger than damping due to collisions and thermal conductivity. Wojaczek had considered only the latter two mechanisms in his calculations, and this explains the discrepancy noted above.

Berlande, Goldan and Goldstein found modulation of the light emitted by an afterglow discharge in a cryogenic plasma. [4] They attribute the acoustic wave production to decay of electron temperature, but present no analysis to support this contention.

Goldstein, Roux, and Dayton introduced a sound wave into a discharge tube by microwave breakdown and heating of the gas at one end. [22] This sound wave was detected by monitoring the variations of quantities in three spearate devices: (1) light intensity in an afterglow plasma located at some distance from this source,(2) microwave power transmitted in a waveguide in which the same afterglow plasma was used as a dielectric post,(3) current in a gas-filled thermionic diode. The latter is explained in Chapter II.

Gentle and Ingard used a high-voltage pulsed breakdown for sound wave production, and biased Langmuir probes into the ion collection region to measure the sonic velocity. In this manner they determined gas temperature in a dc discharge maintained in a flowing gas. [21] Nygaard also used a high-voltage pulse breakdown for sound wave production, observing the arrival of the sound wave by means of a time displacement of the density-sensitive Tonks-Dattner resonances in an after-

glow plasma. [39]

Ingard and Gentle have shown that density variations in the neutral gas will cause corresponding variations in the ion and electron densities. [27] Saxton's work confirmed this. [72] Ingard's later work also shows that acoustic waves may be amplified in the discharge. [26]

Sodha and Palumbo have theoretically analyzed interaction of acoustic and electromagnetic waves in a plasma. [75] They note that electromagnetic waves in the plasma can be modulated by acoustic waves in such cases. Modulation can also occur upon reflection from a plasma-free-space boundary which is affected by an acoustic signal. This can become important in upper atmosphere detection of acoustic waves generated by explosions and rockets.

Strickler and Stewart were in the process of investigating the effect of square-wave modulation of the discharge in connection with moving striations, when they discovered that they had caused the column to assume a permanent kink. [77] This was attributed to the excitation of a normal longitudinal acoustic mode of the column, and is the most striking effect observed so far.

BIBLIOGRAPHY

1. Abria. Annales de Chimie, v. 7, 1843, 462.

2. Achterberg, H. and J. Michel, Some results of moving striations in a neon glow discharge. Annalen der Physik, v. 7. 1959, 365-379.

3. Acton, J. R. and J. D. Swift. Cold Cathode Discharge Tubes. Academic Press, 1963.

4. Berlande, J., P. D. Goldan, and L. Goldstein. Formation and propagation of a pressure wave in a weakly ionized gas. Applied Physics Letters, v. 5, August, 1964, 51-52.

5. Bletzinger, P. and A. Garscadden. Image converter measurements on moving striations. Journal of Electronics and Control, v. 16, 1964, 169-173.

6. Blum, B. W., I. Dyer and U. Ingard. The corona discharge transducer. Journal of the Acoustical Society of America, v. 26, 1954, 139.

7. Briand, J. and J. L. Delcroix. Excitation of acoustic waves by interaction between charged particles and neutral molecules in a discharge tube. Comptes Rendus L'Academie des Sciences, v. 253, 1961, 824-826.

8. Cahn, J. H. Electronic interaction in electrical discharges in gases. Physical Review, v. 75, January 15, 1949, 293-300.

9. Carretta, A. A. Jr. and W. N. Moore. Acoustical observations in a neon glow discharge. United States Naval Postgraduate School. Master's Thesis, 1965.

10. Cooper, A. W. and N. L. Oleson. Critical currents for moving striations in an inert gas. Proceedings of the Fifth International Conference on Ionization Phenomena in Gases, v. 1, 1961, 566-572.

11. Cooper, A. W. Experiments on the origin of moving striations. Journal of Applied Physics, v. 35, 1964, 2877-2884.

12. Cooper, A. W. Moving striations in inert gas glow discharges. Doctoral Dissertation, The Queen's University of Belfast, 1961.

13. Cobine, J. D. Gaseous Conductors, Theory and Applications. McGraw Hill, 1941.

14. Dayton, J. A. Jr., J. T. Verdeyen, and P. F. Virobik. Method for detecting weak sound waves in a low pressure gas. Review of Scientific Instruments, v. 34, December, 1963, 1451-1452.

15. Druyvesteyn, M. J. Calculation of Townsend's α for Ne. Physica, v. 3, 1936, 65-74.

16. Druyvestyn, M. J. and F. M. Penning. The mechanism of electrical discharges in gases at low pressures. Reviews of Modern Physics, v. 12, 1940, 87-174.

17. von Engel, A. Ionized Gases. Clarendon Press, 1965.

18. Eure, S. L. Resonant radiation and moving striations in an argon glow discharge. United States Naval Postgraduate School. Master's Thesis, 1966.

19. Garscadden, A. and Bletzinger. Langmuir probe measurements in the presence of oscillations. Review of Scientific Instruments, v. 35, 1964, 912-913.

20. Garscadden, A. and D. A. Lee. Forward and backward-wave moving striations in the constricted discharge. International Journal of Electronics, v. 20, June 1966, 567-581.

21. Gentle, K. W. and U. Ingard. Determination of neutral gas temperature in a plasma column from sound velocity measurements. Applied Physics Letters, v. 5, 1964, 105-106.

22. Goldstein, L., M. R. Roux and J. A. Dayton, Jr. Production of acoustic waves by R-F. breakdown in low pressure gases. Sixth International Conference on Ionization Phenomena in Gases, v. 3, 115-120.

23. Gurevich, A. V. The influence of collisions between electrons on their velocity distribution in gases and semiconductors in an electric field. Soviet Physics-JETP, v. 10, January, 1960, 215-216.

24. Hall, R. F. and B. J. Stocker. An inert gas glow discharge with low maintaining potential. Proceedings of the Sixth International Conference on Ionization Phenomena in Gases, v. II, 57.

25. Hayess, E. The damping of sound waves in the discharge column of low pressure plasmas. Beitrage aus der Plasmaphysik, v. 5, 1965, 211-219.

26. Ingard, U. and R. W. Gentle. Longitudinal waves in a weakly ionized gas. Physics of Fluids, v. 8, July, 1965, 1396-1397.

27. Ingard, U. Acoustic wave generation and amplification in a plasma. Physical Review, v. 145, May, 1966, 41-46.

28. Kagan, Yu. M. & R. I. Lyagushchenko. Electron energy distribution function in the positive column of a neon discharge. Soviet Physics-Technical Physics, v. 6, October, 1961, 321-324.

29. Kagan, Yu. M. and R. I. Lyagushchenko. Electron energy distribution function in the positive column of a discharge. Soviet Physics-Technical Physics, v. 9, November, 1961, 627-631.

30. Kagan, Y. M. and R. I. Lyagushchenko. Electron velocity distribution, excitation and ionization in the positive column of a neon discharge. Soviet Physics-Technical Physics, v. 7, August, 1962, 134-137.

31. Kagan, Yu. M. and A. D. Khakhaev. The excitation of inert gases in the positive column of a discharge at medium pressures. I. Neon. Optics and Spectroscopy, v. 14, May, 1963, 317-322.

32. Kinsler, L. E. and A. R. Frey. Fundamentals of Acoustics. Wiley and Sons, 1963.

33. Klement'ev V. M. Large-radius hollow cathode with uniform discharge over the cross-section. Instruments and Experimental Techniques, v. 2, October, 1965, 267-270.

34. Krejci, V. and L. Pekarek. Determination of dispersion curve parameters from transient wave. (at press)

35. Landau, L. and E. Lifshitz. Fluid Mechanics. Pergamon Press, 1959.

36. Lee, D. A., P. Bletzinger and A. Garscadden. Wave Nature of moving striations. Journal of Applied Physics, v. 37, January, 1966, 377-387.

37. Loeb, L. B. Basic Processes of Gaseous Electronics. University of California Press, 1961.

38. Novak, M. Spatial period of moving striations as a function of electric field strength in glow discharge. Czechoslovak Journal of Physics, v. B 10, 1960, 954-959.

39. Nygaard, K. J. Observation of sound waves in afterglow plasmas by means of Tonks-Dattner resonances. Physics Letters, v. 20, March, 1966, 370-372.

40. Oleson, N. L. and A. W. Cooper. Waves of stratification and ionization waves. Advances in Electronics and Electron Physics (at press).

41. Pekarek, L. Oscillation phenomena in a glow discharge in neon. Czechoslovak Journal of Physics, v. 4, 1954, 221.

42. Pekarek, L. and O. Stirand. Energy balance in the positive column of a glow discharge. Czechoslovak Journal of Physics, v. 6, 1956, 364-375.

43. Pekarek, L. A theory of the successive production of moving striations in the plasma of inert gases. Czechoslovak Journal of Physics, v. 7, 1957, 533-556.

44. Pekarek, L. Factors affecting the self-excitation of low-frequency oscillations in an electric discharge. Czechoslovak Journal of Physics, v. 8, 1958, 32-45.

45. Pekarek, L. Local excitation of the wave of stratification in the positive column of an electric discharge. Czechoslovak Journal of Physics, v. 8, 1958, 498-499.

46. Pekarek, L. The successive production of striations in a glow discharge in hydrogen. Czechoslovak Journal of Physics, v. 8, 1958, 699-704.

47. Pekarek, L. The influence of external illumination on moving striations in a discharge in neon. Czechoslovak Journal of Physics, v. 8, 1958, 742-744.

48. Pekarek, L. Experimental verification of the theory of the successive production of striations in a glow discharge. Czechoslovak Journal of Physics, v. 9, 1959, 67.

49. Pekarek, L. and M. Novak. A new type of moving striation in neon. Czechoslovak Journal of Physics, v. 9, 1959, 401.

50. Pekarek, L. and M. Novak. Microphysical processes that are the cause of the fast waves of stratification in a neon glow discharge. Czechoslovak Journal of Physics, v. 9, 1959, 641.

51. Pekarek, L. and V. Krejci. The physical nature of the production of moving striations in a D-C discharge plasma. Czechoslovak Journal of Physics, v. B 11, 1961, 729-742.

52. Pekarek, L. The mechanism of the amplification of moving striations in a DC discharge. Czechoslovak Journal of Physics, v. B 12, 1962, 296-307.

53. Pekarek, L. Time production and spatial distribution of space charges in D-C discharge plasma. Czechoslovak Journal of Physics, v. B 12, 1962, 439-449.

54. Pekarek, L. and V. Krejci. Theory of moving striations in plasma of a D-C discharge. I. Basic equation and its general solution. Czechoslovak Journal of Physics, v. B 12, 1962, 450-460.

55. Pekarek, L. and V. Krejci. Diffusion of electrons by temperature gradient in plasma of positive column. Czechoslovak Journal of Physics, v. B 12, 1962, 815-820.

56. Pekarek, L. and V. Krejci. The theory of moving striations in a D-C discharge plasma. II. High current approximation. Czechoslovak Journal of Physics, v. B 13, 1963, 881-894.

57. Pekarek, L. The development of a pulse disturbance in a DC discharge plasma. Sixth International Conference on Ionization Phenomena in Gases. Paris, v. III, 1963, 133-137.

58. Pekarek, L. and K. Masek. Macroscopic space charge field in disturbed quasineutral plasma. Czechoslovak Journal of Physics, v. B 15, 1965, 644-661.

59. Pekarek, L., V. Krejci, O. Stirand and L. Laska. Continuous transition from a backward to a forward ionization wave. Physical Review Letters, v. 15, 1965, 721-722.

60. Pekarek, L. Dispersion of ionization waves in neon-hydrogen mixtures. (at press)

61. Pol, B. Van der, and H. Bremmer. Operational calculus based on the two-sided Laplace integral. Cambridge University Press, 1955.

62. Popovici, C. and M. Somesan. Hollow-cathode discharge in magnetic field. Electronics Letters, v. 1, April, 1965, 31-32.

63. Popovici, C. and M. Somesan. On the emission spectrum of the negative glow plasma of a hollow-cathode discharge in magnetic field. Applied Physics Letters, v. 8, March, 1966, 103-105.

64. Pupp, W. Moving striations in the positive column of noble gases. Physikalische Zeitschrift, v. 33, 1932, 844-847.

65. Pupp, W. The influence of the anode on the stability of the homogeneous plasma column in argon. Physikalische Zeitschrift, v. 34, 1933, 756-761.

66. Pupp, W. Frequency and layer width of moving striations in the positive column of noble gases. Zeitschrift fur Technische Physik, v. 15, 1934, 257-262.

67. Pupp, W. Oscillographic probing measurements on moving striations of the positive column of rare gases. Physikalische Zeitschrift, v. 36, 1935, 61-66.

68. Rutscher, A. and K. Wojaczek. Conditions for oscillation-free low pressure gas discharges. I. General survey. Beitrage aus der Plasmaphysik, v. 4/63, 1963, 217-245.

69. Rutscher, A. and K. Wojaczek. Conditions for oscillation-free low pressure gas discharges. II. Existence range of the positive column without moving striations. Beitrage aus der Plasmaphysik, v. 1-2/64, 1964, 41-59.

70. Ruzicka, T. and L. Pekarek. An exact solution to the theory of the decay of an impulse disturbance in a one-dimensional diffusion plasma. Beitrage aus der Plasmaphysik, v. 3/65, 1965, 161.

71. Saxton, W. A. Observation of sound waves generated by DC discharges. Journal of Applied Physics, v. 36, 1965, 1796-1797.

72. Saxton, W. A. Excitation of acoustic waves in plasmas. Journal of Research of the National Bureau of Standards, v. 69 D, 1965, 609-616.

73. Sicha, M. Influence of a strong high-frequency field on the stratification of a DC glow discharge. Czechslovak Journal of Physics, v. 9, 1959, 495-504.

74. Smit, J. A. Velocity distribution of electrons in helium. Physica, v. 3, 1936, 543-560.

75. Sodha, M. S. and C. J. Palumbo. Modulation of electromagnetic waves by acoustic waves in plasmas. Canadian Journal of Physics, v. 42, August, 1964, 1635-1642.

76. Stirand, O., V. Krejci and L. Laska. A new method of time-space display of wave phenomena in Plasma. Czechoslovak Journal of Physics, v. B16, 1966, 65-66.

77. Strickler, S. D. and A. B. Stewart. Radial and azimuthal standing sound waves in a glow discharge. Physical Review Letters, v. 11, 1963, 527-529.

78. Sturges, D. J. and H. J. Oskam. Studies of the properties of the hollow cathode glow discharge in helium and neon. Journal of Applied Physics, v. 35, October, 1964, 2887-2894.

79. Sturges, D. J. and H. J. Oskam. Hollow cathode glow discharge in hydrogen and the noble gases. Journal of Applied Physics, v. 37, 1966, 2405-2412.

80. Subertova, S. Influence of acoustic waves on positive column of low-pressure discharge. Czechoslovak Journal of Physics, v. B 15, October, 1965, 701-702.

81. Suits, C. G. The determination of arc temperature from sound velocity measurements. I. Physics, v. 6, 1935, 190.

82. Vorob'eva, N. A., Yu. M. Kagan, and V. M. Milenin. Electron distribution function in the positive column of a discharge in neon and in helium. Soviet Physics-Technical Physics, v. 9, May, 1965, 1598-1600.

83. Wilson, O. B. Jr. Observations of acoustic waves generated in a neon glow discharge. Journal of the Acoustical Society of America, v. 39, June, 1966, 1260.

84. Wojaczek, K. Continuous small amplitude layers in the argon low pressure discharge. Acta Physica, v. 11, 1959, 35-45.

85. Wojaczek, K. Simplified diffusion theory of moving striations. Annalen der Physik, v. 7, 1959, 37-47.

86. Wojaczek, K. Small amplitude moving striations in the argon low pressure discharge. Acta Physica Hungary, v. 11, 1960, 35-45.

87. Wojaczek, K. Sound in a low pressure discharge. Beitrage aus der Plasmaphysik, v. 3, 1961, 127.

88. Wojaczek, K. On the theory of moving striations of small amplitude in low pressure discharges. Beitrage aus der Plasmaphysik, v. 2, no. 1, 1962, 1-12.

89. Wojaczek, K. The positive column of the argon low-pressure discharge in the transition region. II. Beitrage aus der Plasmaphysik, v. 2/62, 1962, 13-23.

90. Wojaczek, K. Theory of waves of stratification in low pressure gas discharges. Beitrage aus der Plasmaphysik, v. 2/62, 1962, 49-65.

91. Zaitsev, A. A. Oscillations in the discharge as a source of moving striations. Doklady Akademii Nauk, USSR, v. 79, 1951, 779-781.

INITIAL DISTRIBUTION LIST

		No. Copies
1.	Defense Documentation Center Cameron Station Alexandria, Virginia 22314	20
2.	Library Naval Postgraduate School Monterey, California 93940	2
3.	LT Joel L. Crandall, Jr., USN 8113 Deerfield Drive Norfolk, Virginia 23518	5
4.	Prof. A. W. Cooper Department of Physics Naval Postgraduate School Monterey, California 93940	5
5.	Prof. O. B. Wilson Department of Physics Naval Postgraduate School Monterey, California 93940	1
6.	Mr. Robert Sanders Dept. of Materials Science and Chemistry Naval Postgraduate School Monterey, California 93940	1
7.	Mr. William P. Jones NASA Ames Laboratory Moffett Field, California 94035	1
8.	Commander Naval Ordnance Systems Command Navy Department Washington, D.C. 20360	1
9.	Mr. Peter P. Crooker Department of Physics Naval Postgraduate School Monterey, California 93940	1

DOCUMENT CONTROL DATA - R&D

(Security classification of title, body of abstract and indexing annotation must be entered when the overall report is classified)

1. ORIGINATING ACTIVITY (Corporate author)	2a. REPORT SECURITY CLASSIFICATION
Naval Postgraduate School Monterey, California 93940	UNCLASSIFIED
	2b. GROUP

3. REPORT TITLE

ACOUSTIC PERTURBATION OF A NEON GLOW DISCHARGE

4. DESCRIPTIVE NOTES (Type of report and inclusive dates)

Thesis, Doctor of Philosophy, March 1967

5. AUTHOR(S) (Last name, first name, initial)

CRANDALL, Joel Lee Jr.

6. REPORT DATE	7a. TOTAL NO. OF PAGES	7b. NO. OF REFS
March 1967	121	91

8a. CONTRACT OR GRANT NO.	9a. ORIGINATOR'S REPORT NUMBER(S)
b. PROJECT NO.	
c.	9b. OTHER REPORT NO(S) (Any other numbers that may be assigned this report)
d.	

10. AVAILABILITY/LIMITATION NOTICES

[redacted] 6226 11/69

This document has been approved for public release and sale; its distribution is unlimited.

11. SUPPLEMENTARY NOTES	12. SPONSORING MILITARY ACTIVITY

13. ABSTRACT

Acoustic waves of finite extent were propagated into a dc glow discharge. It was found that compression phases of these waves reduced light emitted by the discharge, while rarefaction phases increased this light. In the compression phase of the acoustic wave these changes were attributed to increased losses of electron energy through an increase in the collision frequency. Electron energy was increased in the rarefaction phase of the acoustic wave as collision frequency was reduced.

Fast and slow waves of stratification were excited by the acoustic waves. These waves of stratification had opposite signs of light intensity variation when excited by compression and rarefaction phases of the acoustic wave.

DD FORM 1 JAN 64 1473

14 KEY WORDS	LINK A		LINK B		LINK C	
	ROLE	WT	ROLE	WT	ROLE	WT
Striations						
Moving Striations						
Ionization Waves						
Acoustic						
Acoustic Interaction						
Glow Discharge						
Diode Microphone						